Molecular Phylogenetics and Evolution 65 (2012) 421–436

Contents lists available at SciVerse ScienceDirect

Molecular Phylogenetics and Evolution

journal homepage: www.elsevier.com/locate/ympev

Acrobat ants go global – Origin, evolution and systematics of the genus *Crematogaster* (Hymenoptera: Formicidae)

Bonnie B. Blaimer

Department of Entomology, University of California-Davis, Davis, CA 95616, USA

ARTICLE INFO

Article history:
Received 6 January 2012
Revised 31 May 2012
Accepted 29 June 2012
Available online 10 July 2012

Keywords:
Crematogaster
Ants
South-East Asia
Madagascar
Transoceanic dispersal
Biogeography

ABSTRACT

This study unravels the evolution and biogeographic history of the globally distributed ant genus *Crematogaster* on the basis of a molecular phylogeny, reconstructed from five nuclear protein-coding genes and a total of 3384 bp of sequence data. A particular emphasis is placed on the evolutionary history of these ants in the Malagasy region. Bayesian and likelihood analyses performed on a dataset of 124 *Crematogaster* ingroup taxa lend strong support for three deeply diverging phylogenetic lineages within the genus: the *Orthocrema* clade, the Global *Crematogaster* clade and the Australo-Asian *Crematogaster* clade. The 15 previous subgenera within *Crematogaster* are mostly not monophyletic. Divergence dating analyses and ancestral range reconstructions suggest that *Crematogaster* evolved in South-East Asia in the mid-Eocene (40–45 ma). The three major lineages also originated in this region in the late Oligocene/early Miocene (~24–30 ma). A first dispersal out of S-E Asia by an *Orthocrema* lineage is supported for 22–30 ma to the Afrotropical region. Successive dispersal events out of S-E Asia began in the early, and continued throughout the late Miocene. The global distribution of *Crematogaster* was achieved by subsequent colonizations of all major biogeographic regions by the *Orthocrema* and the Global *Crematogaster* clade. Molecular dating estimates and ancestral range evolution are discussed in the light of palaeogeographic changes in the S-E Asian region and an evolving ocean circulation system throughout the Eocene, Oligocene and Miocene. Eight dispersal events to/from Madagascar by *Crematogaster* are supported, with most events occurring in the late Miocene to Pliocene (5.0–9.5 ma). These results suggest that *Crematogaster* ants possess exceptional dispersal and colonization abilities, and emphasize the need for detailed investigations of traits that have contributed to the global evolutionary success of these ants.

1. Introduction

Ants are arguably one of the most abundant and ecologically dominant groups of arthropods in the world. They are able to occupy all major habitat types and ecosystems (Wilson and Hölldobler, 2005). Most ant genera, however, have succeeded only in colonizing one or a few biogeographical regions and are fairly restricted in their habitat preferences. Global distribution is rare among ant genera, but the notable exceptions to this rule are often very diverse and species-rich groups that have been ecologically highly successful. Such an example is the focal group of this study, *Crematogaster*. The genus currently comprises 467 nominal species (excluding subspecies; cf. Bolton, 2011) distributed widely in tropical and temperate latitudes, although with a much elevated diversity in subtropical and tropical regions. These ants occur mostly in forest, woodland or savannah habitats, where they inhabit both the ground as well as the canopy level. Most tropical species nest arboreally, in dead branches, under bark or in independent carton nest structures. Ground nesting probably occurs more frequently in temperate areas, and then often under stones – but some species in the tropics also have adapted to leaf litter and soil habitats (Hosoishi et al., 2010). Arboreal species of *Crematogaster* in particular can be dominant elements of the ant fauna, with polydomous and strongly territorial colonies (Blaimer, 2010; Dejean et al., 2010).

As is the case in many other widespread genera, the species-level taxonomy of *Crematogaster* ants is difficult (Brown, 1973; Ward, 2007). Many synonyms and undescribed species likely still exist, although much progress has been made recently (e.g. Blaimer, 2010, 2012a, 2012b; Hosoishi and Ogata, 2009; Longino, 2003). On the genus level, *Crematogaster* is easily recognizable by the unique dorsal attachment of the postpetiole (3rd abdominal segment) to the rest of the metasoma (i.e. the gaster). This feature constitutes the strongest morphological synapomorphy of the genus (Bolton, 2003) and also confers the ability to raise the gaster high over the rest of the body in a defensive posture. Reminding of a balancing act, this behavior gave these ants their common name: acrobat ants. Confronted with an ever-mounting diversity of species through new descriptions, taxonomists have very early on attempted to erect an internal subgeneric classification system for the genus based on morphology. Most of the currently recognized 15 subgenera were established by Forel and Santschi (for details see Blaimer, in press). These subgeneric descriptions mostly did not provide concise and

E-mail addresses: bbblaimer@ucdavis.edu, bonnieblaimer@gmail.com

1055-7903/$ - see front matter © 2012 Elsevier Inc. All rights reserved.
http://dx.doi.org/10.1016/j.ympev.2012.06.028

clear diagnostic character states for identification, and their validity as natural groups in a phylogenetic sense is doubtful.

An equal conundrum is the relationship of *Crematogaster* within the largest subfamily of ants, the Myrmicinae. Bolton (2003) assigned the Asian endemic genus *Recurvidris* to the same tribe, Crematogastrini, on basis of some morphological similarities. Molecular phylogenetic studies have not been able to confirm this, nor any other close relationships with high support (Brady et al., 2006; Moreau et al., 2006; P.S. Ward pers. comm.). Brady et al. (2006) estimated a timeframe for the evolution of the Myrmicinae of ca. 80–90 ma. Within this subfamily, *Crematogaster* is placed in a well supported clade together with other genera between which relationships, however, remain unresolved (P.S. Ward, pers. comm.).

In this study, I examine the global phylogeny and biogeography of the genus *Crematogaster*, with a special focus on the Malagasy fauna. In Madagascar, *Crematogaster* is moderately diverse with 32 known (described and undescribed) species, which fall into several morphological species-groups (and five of the nominal subgenera), whose taxonomy is in the process of revision (Blaimer, 2010, 2012a). Acrobat ants in Madagascar are predominantly arboreal and one of the most conspicuous ant groups in all forest habitats. Species distribution patterns are characterized partly by widespread species found across large parts of the island, and cases of local endemism especially in mountainous regions (Blaimer, unpubl.). All Malagasy *Crematogaster* are endemic to the island, although four species also occur in the greater Malagasy region (including Comoros, Mayotte, Seychelles and the Mascarenes).

Since its last contact with India ca. 80–87 ma during Gondwanan break-up (Storey et al., 1995; Upchurch, 2008), the continental island Madagascar has remained in complete isolation from other landmasses. It is separated from the African mainland by the Mozambique channel, which is at least 430 km wide at its narrowest width. A few small oceanic islands break up this distance, with the most notable in size being the Comoros Islands. Unraveling the geographic origins of Madagascar's hyperdiverse and highly endemic biota has fueled numerous molecular phylogenetic studies. It is nowadays a widely accepted view that most of this unique species diversity has been generated by transoceanic dispersal and subsequent radiations ('neoendemisms'), rather than paleoendemisms with a Gondwanan origin (see review of Yoder and Nowak, 2006). Considering that the subfamily Myrmicinae originated only around the time of Madagascar's separation from India, *Crematogaster* therefore must have also reached the island via transoceanic dispersal. The questions remaining to be investigated are when and from where acrobat ants have colonized Madagascar, and, considering the diversity of morphological species-groups, how many dispersal events have taken place.

In this study, I reconstruct a framework phylogeny for *Crematogaster* ants to improve current understanding of relationships within the genus and to elucidate their global evolutionary and biogeographic history. I hereby first seek to reveal the phylogenetic structure within the genus and investigate whether subgenera represent monophyletic groupings. My second objective is to infer the center of origin for acrobat ants and sketch a time-calibrated picture of their subsequent spread across the world. Thirdly, I comprehensively investigate the biogeography of *Crematogaster* in the Malagasy region to understand their faunal affinities and the timeline of colonization of Madagascar by acrobat ants.

2. Materials and methods

2.1. Taxon sampling

Taxa were selected for this study with the goals of representing the phylogenetic diversity of the whole genus worldwide and the entire Malagasy *Crematogaster* species diversity. I was guided by previous subgeneric assignments and geographic distribution as indicators to select species for molecular sampling, and I attempted to sample subgenera in proportion to their size and distribution. Table 1 provides an overview of the current size and distribution of the subgenera, and indicates the number and distribution of sampled taxa. These numbers were taken from Bolton (2011), while also including some unpublished data on new species and subgeneric transfers (pers. observ.; S. Hosoishi, pers. comm.; H. Feldhaar, pers. comm.). Further included in the study are eight members of other ant genera (*Metapone*, *Vollenhovia*, *Tetramorium*, *Recurvidris*, *Leptothorax*, *Temnothorax*, *Aphaenogaster*, *Stenamma*) within the subfamily Myrmicinae, ranging from moderately to distantly related to *Crematogaster*.

2.2. Species identification and morphological observations

Crematogaster ants are challenging to identify to species level. Most specimens were identified using either reference collections or images, existing identification keys or original species descriptions in the literature. Taxa bearing the label "cf" before the species name were usually identified using literature only. This denotation indicates that identification may not be fully accurate, but that the specimen is expected to have a close morphological affinity to the applied name. Malagasy taxa labeled with code names represent undescribed species, while in cases of taxa from other regions this could mean either "undescribed" or "no identification possible". These codes are not intended to for use in formal nomenclatural purposes.

Color images of voucher specimens were created with a JVC KY-F75U digital camera, a Leica MZ16A stereomicroscope, Syncroscopy Auto-Montage (v5.0) software and Zerene Stacker (v1.02) software. These are publicly available on AntWeb (www.antweb.org). For Malagasy taxa the molecular voucher specimens have not been imaged, but representative images for respective species are available on AntWeb. Species distributions were plotted with ArcMap (v9.3) within the software ArcGIS, based on coordinates (latitude and longitude) as given in the Supplementary Table 1.

2.3. Molecular data collection

DNA was extracted from 124 ingroup specimens using a DNeasy Tissue Kit (Qiagen Inc., Valencia, CA, USA), following the manufacturer's protocol but eluting the extract in sterilized water rather than the supplied buffer and at half the suggested volume. I used primarily a non-destructive method (cuticle pierced prior to extraction), enabling me to retain and re-mount voucher specimens after extractions. In cases where multiple individuals from colony series were available, a destructive technique (entire ant pulverized) was preferred. Five nuclear protein-coding genes were selected for amplification: long wavelength rhodopsin (LW Rh, 856 bp exon /199 bp intron), arginine kinase (ArgK, 390 bp exon), carbamoylphosphate synthase (CAD, 536 bp exon/193 bp intron), wingless (Wg, 409 bp exon) and DNA topoisomerase 1 (Top1, 802 bp exon). Four of these genes are widely used for phylogenetic inference in ants and primers are available (Blaimer, 2012a; Ward and Downie, 2005; Brady et al., 2006; Moreau et al., 2006; Ward et al., 2010), primers for Top1 have recently been published by Ward and Sumnicht (2012). The sequence lengths given here refer to the aligned sequence data included in the matrix used for phylogenetic inference. Amplifications of LW Rh, ArgK, CAD, Top1 and Wg were performed using standard PCR methods outlined in Ward and Downie (2005) and sequencing reactions were analyzed on an ABI 3730 Capillary Electrophoresis Genetic Analyzer with ABI BigDye Terminator v3.1 Cycle Sequencing chemistry (Applied Biosystems Inc., Foster City, CA). Most gene fragments were successfully

Table 1
Taxon sampling. Taxon sampling in relation to previous classification and distribution. AFR = Afrotropical region; AUS = Australasian region; MAD = Malagasy region; NEA = Nearctic region; NEO = Neotropical region; PAE = Palearctic region; SEA = South-East Asia. Numbers refer to number of taxa described/sampled (in bold). Species numbers are based upon Bolton (2011) and unpublished data; only nominal species are included.

Subgenus	Species	Taxa sampled	Distribution: total taxa/sampled taxa
Crematogaster (sensu stricto)	196	50	Global; AFR: 69/**8**, MAD: 17/**17**, SEA: 55/**10**, AUS: 13/**7**, NEO: 9/**1**, NEA: 22/**5**, PAE: 11/**2**
Orthocrema	108	28	Global; AFR: 11/**2**, MAD: 5/**5**, SEA: 18/**8**, AUS: 15/**3**, NEO: 56/**8**, NEA: 2/**1**, PAE: 1/**1**
Decacrema	24	12	AFR: 5/**2**, MAD: 7/**7**, SEA: 11/**3**, AUS: 1/**0**
Oxygyne	22	6	AFR: 8/**2**, MAD: 3/**2**, SEA: 10/**1**, AUS: 1/**1**
Mesocrema	12	3	MAD: 1/**1**, SEA: 6/**2**, AUS: 5/**0**
Sphaerocrema	30	6	AFR: 30/**6**
Atopogyne	16	3	AFR: 16/**3**
Physocrema	12	3	SEA: 12/**3**
Paracrema	5	2	SEA: 5/**2**
Rhachiocrema	5	3	SEA: 1/**0,** AUS: 4/**3**
Xiphocrema	7	3	AUS: 7/**3**
Colobocrema	1	1	SEA: 1/**0**
Neocrema	13	2	NEO: 13/**2**
Eucrema	4	1	NEO: 4/**1**
Unassigned	12	1	NEO: 10/**1**, SEA: 2/**0**
Total taxa	467	**124**	

obtained from all specimens; the total percentage of gaps in the data matrix amounts to 0.67%. 375 bp of alignment-ambiguous or "gap-heavy" sites were excluded from all analyses, and a total of 3384 bp of aligned sequence data was hence used in phylogenetic inference. Some of the sequences for the eight outgroup taxa (Brady et al., 2006) and for a few of the ingroup taxa were already published (Blaimer, 2012a, 2012b); all newly generated sequences have been deposited in GenBank, with accession numbers listed in Table 2. The aligned data matrix and the Bayesian tree (used to produce Fig. 2) have been deposited in TreeBase (ID12251; http://purl.org/phylo/treebase/phylows/study/TB2:S12251).

2.4. Phylogenetic inference

Sequence data were assembled and edited in the program Sequencher 4.6 (Gene Codes Corporation, 2006, Ann Arbor, MI), aligned in Muscle 3.7 (Edgar, 2004) accessed through the CIPRES science gateway (Miller et al., 2010), and unambiguous misalignments were manually realigned in MacClade 4.08 (Maddison and Maddison, 2000). Prior to alignment the intron data from respective sequences in all eight myrmicine outgroup taxa was deleted. The intron data for the ArgK-gene was further discarded entirely from the 132-taxon alignment.

Phylogenetic analyses within a Bayesian inference framework (BI hereafter) were performed using MrBayes v3.1 (Ronquist and Huelsenbeck, 2003), accessed through the CIPRES science gateway (Miller et al., 2010) and the University of Oslo Bioportal (www.bioportal.uio.no); analyses within a maximum likelihood framework (ML) used GARLI v2.0 (Zwickl, 2006) and RAxML-GUIv.0.93 (Stamatakis, 2006), performed on an IMac desktop computer.

BI- and ML-analyses were based on a concatenated data matrix of the five loci. The data matrix was divided into biologically sensible subsets by gene, translational pattern (exon, intron) and codon position, and five partitioning schemes were defined that ranged from simple (*unpart*, *5 part*, *7 part*) to complex (*12part* and *17 part*); these are outlined in Table 3. Best-fitting models of nucleotide sequence evolution were selected for each partition using the Akaike information criterion (AIC) in the program MrModeltest v2.3 (Nylander, 2004; Posada and Crandall, 1998) for application in BI-analyses, and in Modeltest v3.7 (Posada and Crandall, 1998) for specification in ML-analyses, both executed through PAUP∗ 4.0b10 (Swofford, 2000). Details on selected models for each data subset can be found in Table 3. BI was also performed as single locus analyses on each of the five genes separately to examine potential conflicts in genealogy.

BI-analyses each employed two runs of Metropolis-coupled Markov Chain Monte Carlo (MCMCMC) each consisting of four chains (temp = 0.05) and sampling every 500 or 1000 generations. The model parameters transition–transversion ratio, gamma shape, proportion of invariable sites, rate matrix and state frequencies were unlinked across partitions. Initially a variable rateprior was employed to allow for rate variation among partitions and otherwise settings were left at the default options. I assessed convergence of chains and other diagnostic values in the following ways. In Tracer v1.5 (Rambaut and Drummond, 2007) convergence was confirmed visually and mixing of chains by evaluating effective sample size (ESS) values for all parameters. In MrBayes I confirmed that the ASDSF (average standard deviation of split frequencies) had reached values below 0.01 and PSRF (potential scale reduction factor) values had approached 1.0 for all parameters. To assess whether tree topologies were sampled in proportion to their true posterior distribution, I further used the compare, slide and cumulative plotting functions on the "Are-We-There-Yet" (AWTY) online server (Wilgenbusch et al., 2004).

To reach convergence of MCMC chains, good ESS values and plausible parameter estimates for tree length and rate multipliers, it was necessary to follow steps outlined in Ward et al. (2010) to improve BI performance in MrBayes. 1) I placed a shorter prior of 0.01 on the mean branch length (command *brlenspr = unconstrained: exponential*(100)) that more accurately reflected the mean branch length across the tree as estimated in ML-analyses. 2) I applied a moderately informative Dirichlet prior on the rate multipliers (see Ward et al., 2010), reflecting prior expectations that 3rd codon positions and introns evolve faster than 1st and 2nd positions, and 1st faster than 2nd positions. These altered settings returned good convergence and mixing diagnostics after run lengths of 20 million generations for less complex, and 30 million generations for more complex partitioning schemes (*12 part*, *17part*). Trees were summarized as majority-rule consensus trees in MrBayes, after discarding the first 20–25% of samples as burnin.

The relative fit of the five data partitioning schemes was evaluated in a Bayes factor (BF) comparison, an established method to choose between different partitioning strategies for the same dataset (Brown and Lemmon, 2007). Bayes factors were calculated as $\ln(BF_{21}) = [\ln(HM_2) - \ln(HM_1)]$, where HM_1 and HM_2 represent the harmonic means (estimated marginal likelihoods) of the pos-

Table 2
GenBank accession numbers for sequenced taxa and genes.

Crematogaster	Voucher ID	LW Rh	ArgK	CAD	Top1	Wg	Crematogaster	Voucher	LW Rh	ArgK	CAD	Top1	Wg
aberrans	CASENT0193779	JN129955	JN129894	JN129881	JQ326894	JQ326415	*fruhstorferi*	CASENT0193728	JQ326732	JQ326502	JQ326617	JQ326847	JQ326377
abrupta	CASENT0219566	JQ326662	JQ326432	JQ326547	JQ326777	JQ326309	*grevei*	CASENT0457634	JQ326686	JQ326456	JQ326571	JQ326801	JQ326332
aculeata	CASENT0193600	JQ326663	JQ326433	JQ326548	JQ326778	n.a.	*HFmsp10*	CASENT0193611	JQ326687	JQ326457	JQ326572	JQ326802	JQ326333
acuta	CASENT0193650	JQ326664	JQ326434	JQ326549	JQ326779	JQ326310	*hova-complex*	CASENT0058827	JQ326688	JQ326458	JQ326573	JQ326803	JQ326334
agnetis	CASENT0051228	JN129941	JN129888	JN129885	JQ326893	JQ326417	*inflata*	CASENT0193621	JQ326689	JQ326459	JQ326574	JQ326804	JQ326335
ampullaris	CASENT0193577	JQ326665	JQ326435	JQ326550	JQ326780	JQ326311	*ionia*	CASENT0193617	JQ326731	JQ326501	JQ326616	JQ326846	JQ326376
arcuata	CASENT0193084	JQ326955	JQ326924	JQ326936	JQ326897	JQ326414	*irritabilis*	CASENT0193598	JQ326690	JQ326460	JQ326575	JQ326805	JQ326336
baduvi	CASENT0193723	JQ326710	JQ326480	JQ326595	JQ326825	JQ326356	*isolata*	CASENT0193229	JQ326691	JQ326461	JQ326576	JQ326806	JQ326337
binghamii	CASENT0193689	JQ326671	JQ326441	JQ326556	JQ326786	JQ326317	*kelleri*	CASENT0109989	JQ326746	JQ326516	JQ326631	JQ326861	JQ326391
borneensis	CASENT0193115	JQ326672	JQ326442	JQ326557	JQ326787	JQ326318	*lango*	CASENT0090624	JQ326692	JQ326462	JQ326577	JQ326807	JQ326338
castanea	CASENT0193606	JQ326737	JQ326507	JQ326622	JQ326852	JQ326382	*liengmei*	CASENT0193172	JQ326693	JQ326463	JQ326578	JQ326808	JQ326339
cf bequaerti	CASENT0193744	JQ326743	JQ326513	JQ326628	JQ326858	JQ326388	*lineolata*	CASENT0193619	JQ326694	JQ326464	JQ326579	JQ326809	JQ326340
cf buchneri	CASENT0193750	JQ326669	JQ326439	JQ326554	JQ326784	JQ326315	*lobata*	CASENT0193045	JQ326751	JQ326521	JQ326636	JQ326866	JQ326396
cf chlorotica	CASENT0415414	JQ326730	JQ326500	JQ326615	JQ326845	n.a	*longipilosa*	CASENT0193780	JQ326948	JQ326918	JQ326934	JQ326900	JQ326428
cf concava	CASENT0193755	JQ326723	JQ326493	JQ326608	JQ326838	JQ326369	*longispina*	CASENT0193767	JQ326695	JQ326465	JQ326580	JQ326810	JQ326341
cf cylindriceps	CASENT0193916	JQ326676	JQ326446	JQ326561	JQ326791	JQ326322	*lunaris*	CASENT0110578	JQ326748	JQ326518	JQ326633	JQ326863	JQ326393
cf depressa	CASENT0087590	JQ326667	JQ326437	JQ326552	JQ326782	JQ326313	*madagascariensis*	CASENT0193580	JQ326749	JQ326519	JQ326634	JQ326864	JQ326394
cf desperans	CASENT0193107	JQ326745	JQ326515	JQ326630	JQ326860	JQ326390	*madecassa*	CASENT0068164	JQ326949	JQ326913	JQ326932	JQ326886	JQ326421
cf dolens	CASENT0193756	JQ326956	JQ326923	JQ326940	JQ326898	JQ326426	*mahery*	CASENT0193469	JQ326696	JQ326466	JQ326581	JQ326811	JQ326342
cf excisa	CASENT0193753	JQ326733	JQ326503	JQ326618	JQ326848	JQ326378	*malala*	CASENT0421136	JQ326697	JQ326467	JQ326582	JQ326812	JQ326343
cf ferrarii	CASENT0193918	JQ326673	JQ326443	JQ326558	JQ326788	JQ326319	*marioni*	CASENT0193063	JQ326698	JQ326468	JQ326583	JQ326813	JQ326344
cf gabonensis	CASENT0193595	JQ326668	JQ326438	JQ326553	JQ326783	JQ326314	*meijerei*	CASENT0193683	JN129927	JN129887	JN129852	JQ326890	JQ326419
cf gavapiga	CASENT0193609	JQ326711	JQ326481	JQ326596	JQ326826	JQ326357	*mesonotalis*	CASENT0193622	JQ326700	JQ326470	JQ326585	JQ326815	JQ326346
cf gerstaeckeri	CASENT0193739	JQ326741	JQ326511	JQ326626	JQ326856	JQ326386	*mjobergi*	CASENT0193799	JQ326728	JQ326498	JQ326613	JQ326843	JQ326374
cf latuka	CASENT0193741	JQ326739	JQ326509	JQ326624	JQ326854	JQ326384	*modiglianii*	CASENT0193575	JQ326701	JQ326471	JQ326586	JQ326816	JQ326347
cf luctans	CASENT0193747	JQ326724	JQ326494	JQ326609	JQ326839	JQ326370	*mpanjono*	CASENT0056947	JQ326947	JQ326910	JQ326929	JQ326888	JQ326424
cf ochracea	CASENT0193607	JQ326734	JQ326504	JQ326619	JQ326849	JQ326379	*nigropilosa*	CASENT0193769	JQ326703	JQ326473	JQ326588	JQ326818	JQ326349
cf rogenhoferi	CASENT0193596	JQ326735	JQ326505	JQ326620	JQ326850	JQ326380	*nosibeensis*	CASENT0421564	JQ326704	JQ326474	JQ326589	JQ326819	JQ326350
cf rufigena	CASENT0193746	JQ326742	JQ326512	JQ326627	JQ326857	JQ326387	*obnigra*	CASENT0193112	JQ326705	JQ326475	JQ326590	JQ326820	JQ326351
cf laeviceps	CASENT0193616	JQ326725	JQ326495	JQ326610	JQ326840	JQ326371	*onusta*	CASENT0193714	JQ326706	JQ326476	JQ326591	JQ326821	JQ326352
cf wasmanni	CASENT0193947	JQ326666	JQ326436	JQ326551	JQ326781	JQ326312	*opaca*	CASENT0193770	JQ326707	JQ326477	JQ326592	JQ326822	JQ326353
coarctata	CASENT0193116	JQ326675	JQ326445	JQ326560	JQ326790	JQ326321	ortho_CAR1	CASENT0414275	JQ326709	JQ326479	JQ326594	JQ326824	JQ326355
coriaria	CASENT0193778	JQ326677	JQ326447	JQ326562	JQ326792	JQ326323	ortho_TH1	CASENT0130762	JQ326699	JQ326469	JQ326584	JQ326814	JQ326345
corvina	CASENT0193759	JQ326678	JQ326448	JQ326563	JQ326793	JQ326324	*osakensis*	CASENT0193877	JQ326713	JQ326483	JQ326598	JQ326828	JQ326359
dahlii	CASENT0193602	JQ326679	JQ326449	JQ326564	JQ326794	JQ326325	*paradoxa*	CASENT0193114	JQ326714	JQ326484	JQ326599	JQ326829	JQ326360
decamera	CASENT0193613	JQ326680	JQ326450	JQ326565	JQ326795	JQ326326	*pilosa*	CASENT0193165	JQ326715	JQ326485	JQ326600	JQ326830	JQ326361
degeeri	CASENT0012764	JQ326755	JQ326525	JQ326640	JQ326870	JQ326400	*quadriformis*	CASENT0193881	JQ326702	JQ326472	JQ326587	JQ326817	JQ326348
dentata	CASENT0193394	JQ326752	JQ326522	JQ326637	JQ326867	JQ326397	*ranavalonae*	CASENT0193425	JN129942	JN129891	JN129871	JQ326892	JQ326418
emeryi	CASENT0193805	JQ326681	JQ326451	JQ326566	JQ326796	JQ326327	*rasoherinae*	CASENT0070841	JQ326941	JQ326922	JQ326941	JQ326884	JQ326427
flava	CASENT0193691	JQ326682	JQ326452	JQ326567	JQ326797	JQ326328	*razana*	CASENT0193589	JQ326952	JQ326915	JQ326938	JQ326885	JQ326423
flaviventris	CASENT0193696	JQ326744	JQ326514	JQ326629	JQ326859	JQ326389	*reticulata*	CASENT0193610	JQ326712	JQ326482	JQ326597	JQ326827	JQ326358
flavomicrops	CASENT0193764	JQ326683	JQ326453	JQ326568	JQ326798	JQ326329	rhachio_PNG2	CASENT0193603	JQ326717	JQ326487	JQ326602	JQ326832	JQ326363
formosa	CASENT0193615	JQ326684	JQ326454	JQ326569	JQ326799	JQ326330	*rothneyi*	CASENT0193801	JQ326718	JQ326488	JQ326603	JQ326833	JQ326364
fraxatrix	CASENT0193576	JQ326736	JQ326506	JQ326621	JQ326851	JQ326381	*sabatra*	CASENT0193162	JQ326719	JQ326489	JQ326604	JQ326834	JQ326365
fritzi	CASENT0193803	JQ326685	JQ326455	JQ326570	JQ326800	JQ326331	*sagei*	CASENT0193692	JQ326716	JQ326486	JQ326601	JQ326831	JQ326362
sewellii	CASENT0193579	JQ326747	JQ326517	JQ326632	JQ326862	JQ326392	*santschii*	CASENT0193640	JN129924	JN129889	JN129849	JQ326895	JQ326416
sisa	CASENT0127554	JQ326721	JQ326491	JQ326606	JQ326836	JQ326367	*scutellaris*	CASENT0193796	JQ326720	JQ326490	JQ326605	JQ326835	JQ326366
smithi	CASENT0193697	JQ326722	JQ326492	JQ326607	JQ326837	JQ326368	*ss23_loy*	CASENT0125705	JQ326760	JQ326530	JQ326645	JQ326875	JQ326405
sordidula	CASENT0193797	JQ326944	JQ326919	JQ326944	JQ326899	JQ326429	*ss24_rano*	CASENT0492850	JQ326761	JQ326531	JQ326646	JQ326876	JQ326406
ss_AUS2	CASENT0193618	JQ326726	JQ326496	JQ326611	JQ326841	JQ326372	*stadelmanni*	CASENT0193573	JN129928	JN129896	JN129880	JQ326891	JQ326420
ss_AUS3	CASENT0193798	JQ326727	JQ326497	JQ326612	JQ326842	JQ326373	*subcircularis*	CASENT0193915	JQ326762	JQ326532	JQ326647	JQ326877	JQ326407
ss_AUS5	CASENT0193800	JQ326729	JQ326499	JQ326614	JQ326844	JQ326375	*subnuda*	CASENT0193690	JQ326763	JQ326533	JQ326648	JQ326878	JQ326408
ss_TH1	CASENT0119409	JQ326738	JQ326508	JQ326623	JQ326853	JQ326383	*sumichrasti*	CASENT0193773	JQ326764	JQ326534	JQ326649	JQ326879	JQ326409
ss_TZ2	CASENT0193745	JQ326740	JQ326510	JQ326625	JQ326855	JQ326385	*telolafy*	CASENT0492527	JQ326951	JQ326917	JQ326935	JQ326887	JQ326422
ss07_kba	CASENT0148695	JQ326750	JQ326520	JQ326635	JQ326865	JQ326395	*tenuicula*	CASENT0193774	JQ326765	JQ326535	JQ326650	JQ326880	JQ326410

Table 2 (*continued*)

Crematogaster	Voucher ID	LW Rh	ArgK	CAD	Top1	Wg	Crematogaster	Voucher	LW Rh	ArgK	CAD	Top1	Wg
ss10_atbao	CASENT0193221	JQ326753	JQ326523	JQ326638	JQ326868	JQ326398	*tetracantha*	CASENT0193113	JQ326766	JQ326536	JQ326651	JQ326881	JQ326411
ss11_ahe	CASENT0193399	JN129960	JN129920	JN129884	JQ326896	JQ326430	*torosa*	CASENT0193195	JQ326674	JQ326444	JQ326559	JQ326789	JQ326320
ss15_mva	CASENT0120279	JQ326754	JQ326524	JQ326639	JQ326869	JQ326399	*treubi*	CASENT0193783	JQ326767	JQ326537	JQ326652	JQ326882	JQ326412
ss18_anka	CASENT0193039	JQ326756	JQ326526	JQ326641	JQ326871	JQ326401	*victima*	CASENT0193878	JQ326708	JQ326478	JQ326593	JQ326823	JQ326354
ss19_mal	CASENT0021958	JQ326757	JQ326527	JQ326642	JQ326872	JQ326402	*volamena*	CASENT0162194	JQ326946	JQ326912	JQ326931	JQ326889	JQ326425
ss21_avy	CASENT0058825	JQ326758	JQ326528	JQ326643	JQ326873	JQ326403	*weberi*	CASENT0193599	JQ326768	JQ326538	JQ326653	JQ326883	JQ326413
ss22_isa	CASENT0491124	JQ326759	JQ326529	JQ326644	JQ326874	JQ326404	*wellmani*	CASENT0193751	JQ326670	JQ326440	JQ326555	JQ326785	JQ326316
Outgroup	Voucher	LW Rh	ArgK	CAD	Top1	Wg	Outgroup	Voucher	LW Rh	ArgK	CAD	Top1	Wg
Aphaenogaster occidentalis	CASENT0106090	JQ326769	JQ326539	JQ326539	JQ326901	AY867435	Leptothorax cf muscorum	CASENT0106029	JQ326775	JQ326544	JQ326544	JQ326905	EF013710
Stenamma dyscheres	CASENT0106023	JQ326772	JQ326540	JQ326540	JQ326902	EF013772	Temnothorax rugatulus	CASENT0106025	JQ326770	JQ326545	JQ326545	JQ326907	EF013778
Vollenhovia emeryi	CASENT0010125	JQ326773	JQ326546	JQ326546	JQ326904	EF013785	Tetramorium validiusculum	CASENT0106004	JQ326776	JQ326543	JQ326543	JQ326906	EF013781
Metapone madagascarica	CASENT0004528	JQ326774	JQ326541	JQ326541	JQ326903	EF013720	Recurvidris_TH01	CASENT0131659	JQ326771	JQ326542	JQ326542	JQ326908	JQ326431

terior sample of likelihoods from the two respective partitioning strategies under comparison (Nylander et al., 2004). Marginal ln likelihoods and standard error was calculated from four independent runs for each partitioning scheme in Tracer v1.5. Significance of BF values was evaluated using standard tables in the literature (Kass and Raftery, 1995; Nylander et al., 2004). In GARLI, I employed identical partitioning strategies as in MrBayes to perform maximum likelihood searches for the best scoring tree, leaving program configuration settings at defaults. The main motivation for this was to obtain likelihood estimates for branch lengths and total tree lengths independent of results from problematic MrBayes analyses. The Akaike information criterion (AIC) was further utilized as an indicator to choose the best fitting partitioning strategy within the ML framework (McGuire et al., 2007; Li et al., 2008). AIC scores were calculated as $AIC_i = -2\ln L_i + 2k_i$, where L_i is the maximum likelihood of the model and k_i the total number of parameters in the model i; AIC_C was used instead when the ratio of the number of nucleotides to the number of parameters $n/k_i \leqslant 40$ (*12part* and *17part*) to correct for small sample size (Burnham and Anderson, 2002). The AIC_C was calculated as $AIC_{Ci} = -2\ln L_i + 2k_i + 2k_i\,(k_i + 1)/(n - k_i - 1)$.

Bootstrapping was performed in RAxML, using a joint 'thorough bootstrapping' procedure with 100 replicates and ML search for the best tree. RAxML applied a GTRGAMMA model uniformly to all partitions.

2.5. Divergence dating analyses

Divergence dating estimations in this study were implemented in BEAST v.1.6.2 (Drummond and Rambaut, 2007) and applied a lognormal uncorrelated relaxed clock model and a Yule tree prior. Calibrated nodes (see below) were constrained to monophyly, and a UPGMA starting tree, generated in PAUP* (Swofford, 2000), was specified to prevent conflicts of the starting tree with node calibrations. The data were partitioned according to the *17part* scheme, and initially identical substitution models as in MrBayes analyses were employed for each partition. However, results from runs under this partition strategy continued to receive low ESS values for the prior and posterior distribution (and other parameters) even when increasing chain lengths up to 100 million generations. This issue also occurred under the less complex partition schemes *12part* and *7part*. I solved this by changing the substitution model from *gtr* to *hky* in all respective partitions, thereby applying a less complex model with fewer parameters to estimate from the very small data partitions. This returned good parameter estimates for most parameters after 30 million generations, and did not alter posterior age distributions noticeably. All results presented in the following are based on the *17part* – scheme specifying a *hky* model for each partition, and involved two independent runs of MCMC chains sampling for 30 million generations. Parameter- and tree-files were combined in LogCombiner v.1.6.2 (BEAST package, Drummond and Rambaut, 2007), after assessing convergence as above described, and trees were summarized as maximum clade credibility trees in TreeAnnotator v1.6.2 (BEAST package, Drummond and Rambaut, 2007).

Four nodes within the phylogeny were calibrated with prior age distributions to enable estimation of divergence times under the uncorrelated relaxed clock model. For more detailed descriptions of these calibrations see Supplementary data 2.

1) *Stenamma berendti* Mayr, a Baltic amber fossil, ca. 42 ma (Dlussky, 1997). A lognormal prior distribution was assigned with values of 42, 49.4 and 58.8, representing a hard lower bound, median and 95% soft upper bound respectively (input values: *zero offset*: *42, mean: 2.0* and *SD: 0.5*).

Table 3
Data partitions, models and character statistics. Data partitions, models and character statistics of the molecular sequence data matrix. Models of evolution suggested by MrModeltest v2.3 were implemented in MrBayes analyses, while models selected by Modeltest v.3.7 were specified in GARLI.

Data subset	5 part	7 part	12 part	17 part	No. bases	No. VC	No. PIC	Substitution model	
								MrModeltest	Modeltest
LW Rh	x				1055	124	260	HKY + I + G	TrN + I + G
LW Rh exons		x			856	79	176	GTR + I + G	GTR + I + G
LW Rh exons position 1				x	285	24	35	GTR + I + G	GTR + I + G
LW Rh exons position 2				x	285	5	11	GTR + I + G	GTR + I + G
LW Rh exons position 3			x	x	286	50	130	HKY + G	TVM + G
LW Rh exons position 1 + 2			x		570	29	46	GTR + I + G	TVM + I + G
LW Rh introns		x	x	x	199	45	84	GTR + G	TVM + G
ArgK	x	x			390	34	92	HKY + I + G	TrN + I + G
ArgK exon position 1				x	130	9	14	GTR + I	TrN + I
ArgK exon position 2				x	130	6	5	GTR + I	GTR + I
ArgK exon position 3			x	x	130	19	73	GTR + G	TrN + G
ArgK exon position 1 + 2			x		260	15	19	K80 + I + G	TrNef + I + G
CAD	x				729	102	216	HKY + I + G	TrN + I + G
CAD exons		x			536	60	140	HKY + I + G	TrN + I + G
CAD exons position 1				x	178	17	31	HKY + G	TrN + G
CAD exons position 2				x	179	11	14	HKY + G	TrN + G
CAD exons position 3			x	x	179	32	95	HKY + G	HKY + G
CAD exons position 1 + 2			x		357	28	45	HKY + I + G	K81uf + I + G
CAD introns		x	x	x	193	42	76	GTR	TVM + I
Top1									
Top1 exon position 1				x	267	15	19	GTR + I + G	GTR + I + G
Top1 exon position 2				x	267	4	14	HKY + I + G	HKY + I + G
Top1 exon position 3			x	x	268	40	161	GTR + G	GTR + G
Top1 exon position 1 + 2			x		534	19	33	GTR + I + G	TIM + I + G
Wg	x	x			409	30	85	K80 + G	K81 + G
Wg exon position 1				x	136	3	5	GTR + I	GTR + I
Wg exon position 2				x	136	3	5	K80 + I	K80 + I
Wg exon position 3			x	x	137	24	75	GTR + G	GTR + G
Wg exon position 1 + 2			x		272	6	10	GTR + I + G	TIM + I + G
All genes combined (unpart)					3385	349	847	GTR + I + G	GTR + I + G

2) *Temnothorax* spp. in Baltic amber (Dlussky, 1997); a lognormal prior distribution was assigned to this node with values of 42, 49.4 and 58.8 (*42, 2.0, and 0.5*).
3) *Crematogaster crinosa*-group sp. in Dominican amber, ca. 17–20 ma. I assigned three different lognormal prior distribution to this node that together explore the biologically plausible age range for the MRCA of a stem *C. crinosa*-group: A) 17, 20.3 and 25.2 (input values: *zero offset*: *17*, *mean: 1.2* and *SD: 0.55*), B) 17, 25.2 and 30.4 (*17, 2.1* and *0.3*) and C) 17, 30.5 and 35.7 (*17, 2.6* and *0.2*).
4) Myrmicinae subclade containing *Crematogaster* and all outgroups except *Stenamma* and *Aphaenogaster*. A secondary calibration representing the crown-group age range for this clade as estimated in Brady et al. (2006) (S. Brady, pers. comm.; age for this node not published). I here assigned a normal distribution with lower bound = 56.6 ma and upper bound = 68.3 ma (input values: *mean: 62.45* and *SD: 3.45*).

Prior calibration densities can greatly influence posterior age estimations (Ho and Phillips, 2009; Yang and Rannala, 2006). Recently it was further reported that effective prior calibration densities can diverge from the calibration prior distributions defined by the investigator, especially when multiple overlapping calibrations are employed (Heled and Drummond, 2012; Warnock et al., 2011). I therefore performed analyses on empty alignments for each calibration scheme, sampling from the prior only, and compared these results to posterior distributions estimated on sequence alignments. I also assessed the influence of each of the node calibrations on posterior age estimates by running analyses that sequentially excluded each of the four calibrations (results not presented). Presented are results from analyses under three different calibration schemes, varying the prior age density on calibration 3 as outlined above.

To estimate lineage diversification within a temporal context, lineage through time analysis was performed in the program TRACER v1.5 (Rambaut and Drummond, 2007), using results from BEAST analyses under calibration scheme 3B. Results are displayed as lineage-through-time plot, where the solid line corresponds to the mean of the posterior probability density and the shaded area represents the 95% credible interval.

2.6. Biogeographic inference

To model ancestral distributions across the *Crematogaster* phylogeny, I established seven biogeographic regions that best represent the broadest known distributions for extant taxa: A) Palearctic, B) Afrotropical, C) Malagasy, D) South-East Asian, E) Australasian, F) Nearctic and G) Neotropical. Regions D and E are separated along the Wallace line (Lomolino et al., 2005). Fig. 1 gives an overview of extension and boundaries. All taxa were coded for these ranges based on their (known) distribution records. Inference of ancestral geographic ranges was performed in the program LAGRANGE v20110117 (Ree et al., 2005; Ree and Smith, 2008).

LAGRANGE implements a dispersal–extinction–cladogenesis (DEC hereafter) model to infer ancestral ranges for groups of species, and presents results as ancestral range inheritance scenarios for each internal node of the phylogeny. An advantage of this parametric method compared with 'traditional' available parsimony-based methods in biogeography (e.g. dispersal–vicariance-analysis; Ronquist, 1997) is that it can incorporate temporal information (i.e. branch lengths of the tree), and contemporary or historical geological

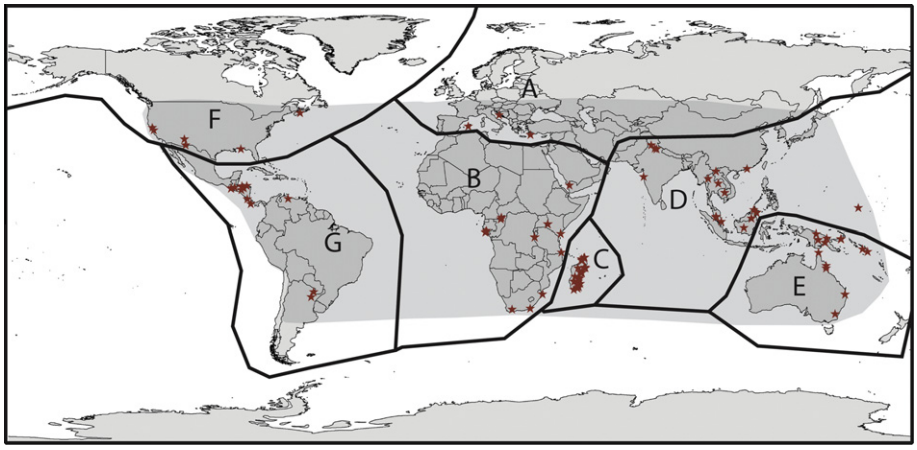

Fig. 1. Generic distribution, taxon sampling and biogeographical regions. Shaded area delineates the distribution of the genus Crematogaster (after Guénard et al., 2010). Red stars mark geographic origin of 124 ingroup specimens; coordinates can be found in Table S1. Bold black lines demarcate the biogeographical regions used for ancestral range reconstructions; A: Palearctic, B: Afrotropical, C: Malagasy, D: South-East Asia, E: Australia and Papua New Guinea, F: Nearctic, G: Neotropical region.

information that may have facilitated or prevented movements of species between range domains (e.g. continental separation or land-bridge connections). Incorporating this information requires users to build a model specifying dispersal scale factors between ranges that are specifically tailored to their data.

For all estimations in LAGRANGE I used the maximum clade credibility tree inferred by BEAST with medium age priors (B) on calibration 3 (see Section 2.5). With the LAGRANGE web configurator (www.reelab.net/lagrange) I constructed two input scripts that incorporated different models with varying scale factors for transition probabilities to experiment with the effect of these values on the inferred ancestral ranges. In both models I constrained the number of ancestral ranges to two, since no extant *Crematogaster* species is known to inhabit more than two of the defined regions and it seems unlikely that ancestral species previously had wider ranges. I further excluded five of the most disjunct ancestral range combinations from the analyses (AC, AE, AG, CF, CG). Both of these measures reduced computational cost. The first model (M1) included otherwise no constraints or alterations from the default values, and all scale transition probabilities were left at 1.0. The M1 model is obviously not very realistic, since it treats over water long-distance dispersal events as equally probable as dispersal events between immediately adjacent regions. In the second model (M2), I adjusted scale values according to the geographic proximity of the ranges, thereby separating (1) pairs of connected, adjacent regions (scale value = 1.0), (2) adjacent regions that are separated through a water barrier (=0.5), and (3) long-distance dispersal where movement between disjunct regions would involve the crossing of an extensive water barrier (=0.1). This resulted in a dispersal matrix as shown in Table 4.

Table 4
Dispersal scale matrix. Dispersal scale matrix implemented in the DEC-M2 model in LAGRANGE. A: Palearctic, B: Afrotropical, C: Malagasy, D: South-East Asia, E: Australasian, F: Nearctic, G: Neotropical region. 1 = high probability of dispersal between regions, chosen for connected landmasses; 0.5 = medium probability of long-distance dispersal between regions, chosen for landmasses in closer proximity that are separated by an oceanic barrier (e.g. Malagasy and Afrotropical regions); 0.01 = low probability of dispersal between regions, chosen for distant regions separated by a wide oceanic barrier (e.g. Neotropics and Malagasy).

Range	A	B	C	D	E	F	G
A	/	1	0.01	1	0.01	0.5	0.01
B	1	/	0.5	1	0.01	0.01	0.01
C	0.01	0.5	/	0.01	0.01	0.01	0.01
D	1	1	0.01	/	0.5	0.01	0.01
E	0.01	0.01	0.01	0.5	/	0.01	0.01
F	0.5	0.01	0.01	0.01	0.01	/	0.5
G	0.01	0.01	0.01	0.01	0.01	0.5	/

3. Results

3.1. Phylogenetic inference

3.1.1. Topology

Both the Bayes factor analysis and the Akaike information criterion chose the most complex (*17part*) partitioning scheme as best fitting to the dataset. Therefore only results from analyses based on this scheme are presented.

Topology remains overall stable across the different types of analyses, and results from ML and BEAST analyses do not notably deviate from the illustrated MrBayes phylogeny (Fig. 2). Notable exceptions are the following major topological rearrangements, both in clade I (i.e. *Orthocrema* clade). A clade containing *C. mesonotalis*, *C. paradoxa*, *C. emeryi* and *C. rachio_PGN2* (node 67 in Fig. 3 and 5) is weakly supported as sister lineage to the rest of clade I in MrBayes (Fig. 2) and ML results (not shown). BEAST analyses (Fig. 3 and 5) in contrast infer this lineage as nested within clade I with moderate PP support (0.92; Supplementary Table 2). The second disagreement between inference methods concerns relationships of the Malagasy species *C. rasoherinae*, *C. mpanjono*, *C. volamena*, *C. razana*, *C. madecassa* and *C. telolafy* to the African species *C. cf dolens* and *C. ortho_CAR1*. The relative positions of these species to each other change across MrBayes (see Fig. 2), BEAST (Fig. 3 and 5) and ML analyses, and the respective nodes receive low support. These topological uncertainties have effects on biogeographic inference that are discussed in Section 3.2.3.1. Clades that receive maximum support (PP = 1.0) with the two Bayesian methods usually also receive high ML-bootstrap support.

3.1.2. Implications for subgeneric classification

All Bayesian (MrBayes and BEAST) and ML-analyses strongly support the genus *Crematogaster* as monophyletic. The genus is subdivided into three deeply divergent clades (I, II, III, Fig. 2), which are further structured into a number of well-supported subclades. Traditional subgeneric groupings are mapped onto the phylogeny in Fig. 2. Clade I consists of taxa that were previously assigned to the subgenera *Orthocrema*, *Neocrema*, *Eucrema*, *Rhachiocrema* and *Mesocrema* (in part) and is hereafter referred to as the "*Orthocrema* clade". Clade II, hereafter called the "Global *Crematog-*

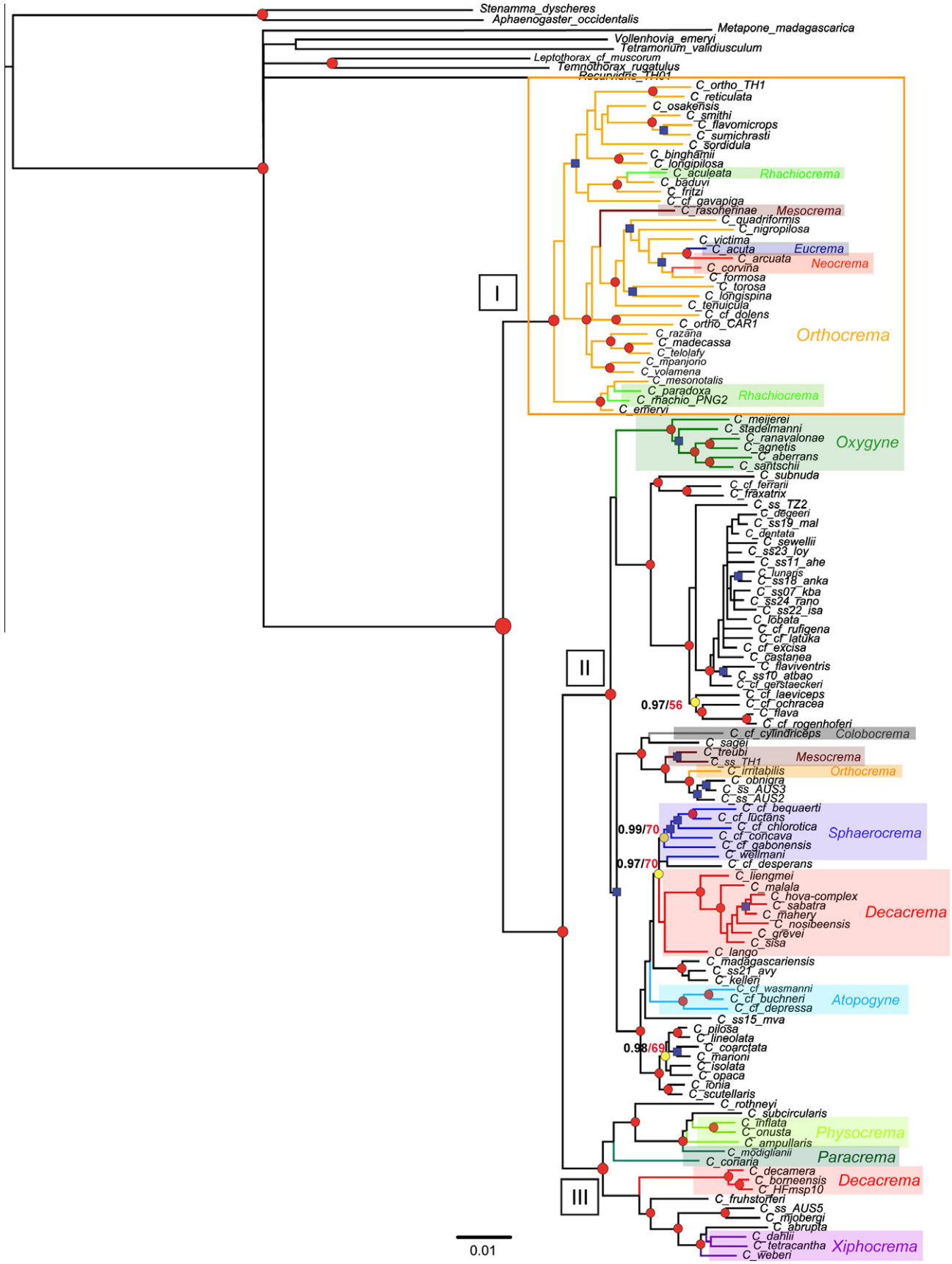

Fig. 2. Phylogeny of *Crematogaster* reconstructed by MrBayes. A consensus tree resulting from analyses based on 3384 bp from LW Rh, ArgK, CAD, Top1 and Wg, summarized across four independent runs with each 30 million generations. The distribution on the tree of the previous 15 subgenera is indicated; taxa not highlighted either belong to *Orthocrema* (framed in orange box) or *Crematogaster sensu* stricto (unframed). Red circles indicate PP = 1.0 and bootstrap > 94; blue squares indicate PP > 0.94 < 1.0 and bootstrap > 74 ⩽ 94; yellow circles indicate where bootstrap ⩽ 74 and PP > 0.94, in these cases both values are shown. Clade labels indicate I: *Orthocrema* clade, II: Global *Crematogaster* clade, III: Australo-Asian *Crematogaster* clade.

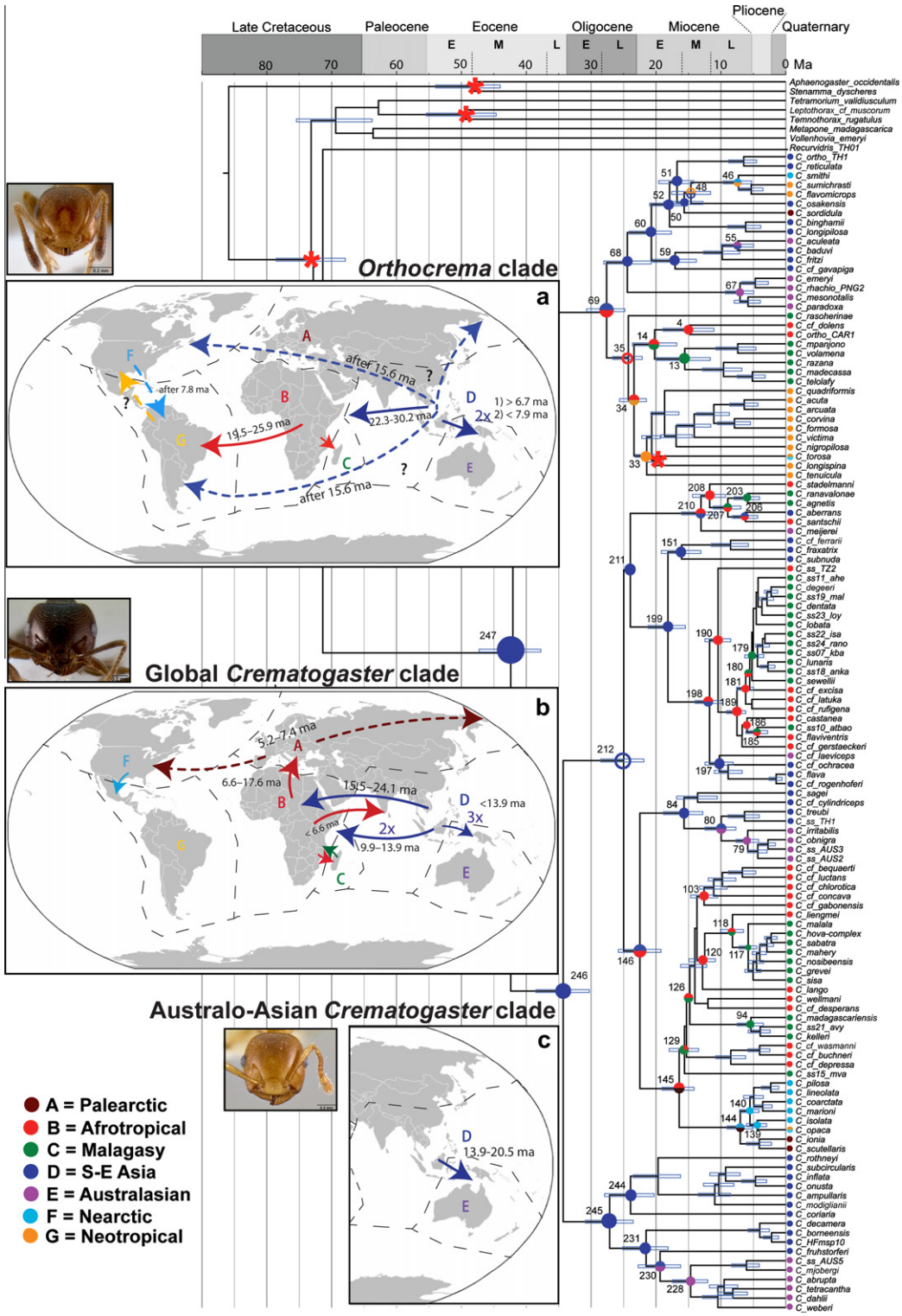

Fig. 3. Biogeographic history of *Crematogaster* inferred by LAGRANGE (DEC-M2). Maximum clade credibility tree inferred by BEAST based on 3384 bp from LW Rh, ArgK, CAD, Top1 and Wg, using calibration scheme 3B (see Section 2.5). Results have been combined from two analyses with 30 million generations. Bars on internal nodes represent error bars for divergence age estimates; red asterisks mark calibrated nodes. Numbers shown beside nodes represent labels assigned to each node during ancestral range reconstructions, and correspond with node numbering in Table 5 and S3; for branch support values (PP; not depicted) refer to Table S3. Ancestral range inheritance scenarios estimated by the dispersal–extinction–cladogenesis model 2 with the highest relative probability (rP) have been mapped on the respective internal nodes (only nodes discussed in the text are shown). Color coding of nodes corresponds with color coding of ranges in diagrams a, b and c, and with the legend in the bottom-left corner. Ranges are A: Palearctic; B: Afrotropical; C: Malagasy; D: South-East Asia; E: Australasian; F: Nearctic; G: Neotropical. Full circles indicate rP $\geqslant$ 0.5, open circles rP < 0.5. Single colored circles mean that both lineages diverging from the respective node inherited the same range. Split circles with two colors (i.e. ranges) mean that the lineages inherited different ranges, and thus indicate a dispersal into a new region. DE on node 80 for example means that one lineage remained in S-E Asia, while the other dispersed to Australasia. Node 129 represents a single case where one lineage is inheriting two ranges (BC). Terminal nodes represent present day ranges of the respective species. Diagrams a, b and c summarize inferred dispersal histories and their timeframes for the *Orthocrema*, Global *Crematogaster* and Australo-Asian *Crematogaster* clade, respectively. Arrows indicate dispersal between regions and are color coded by source; ages represent ranges of median estimates from schemes A-C for calibration 3 (see Table S3).

aster clade", contains *Crematogaster* "sensu stricto" (in part), *Oxygyne*, *Sphaerocrema*, *Atopogyne*, *Decacrema* (in part), *Mesocrema* (in part) and *Colobocrema*. Both of these clades have a global distribution. Clade III in contrast consists only of taxa from the subgenera *Crematogaster* "sensu stricto" (in part), *Decacrema* (in part), *Physocrema*, *Paracrema* and *Xiphocrema* that all occur in South-East Asia, New Guinea and Australia. This clade is therefore named "Australo-Asian *Crematogaster* clade". These three broad lineages within *Crematogaster* are recovered also in single-gene analyses.

Only the subgenera *Oxygyne* and *Atopogyne* are fully supported as monophyletic groups within the current species sampling. The species-rich subgenus *Orthocrema* is paraphyletic, containing a number of smaller subgenera (*Neocrema*, *Eucrema*, *Rhachiocrema*, and part of *Mesocrema*). A few of its members had further been misplaced in other subgenera (see Fig. 2). The largest subgenus, *Crematogaster* sensu stricto has members dispersed across clade II and III of the phylogeny. *Decacrema* was previously thought one of the better supported groupings given a distinct antennal character (10 vs. 11 segments in the rest of the genus), but is here shown as divided into unrelated African and Asian clades. Members of the smaller Asian endemic subgenera *Physocrema*, *Paracrema* and *Xiphocrema* seem to be fairly closely related, but are nonetheless paraphyletic; the same is true for the African endemic group *Sphaerocrema*.

Overall these results support the introduction of significant changes to the subgeneric classification system. However, the formal revision of the subgeneric classification of *Crematogaster* is not subject of this paper and is presented elsewhere (Blaimer, in press).

3.2. Divergence dating and biogeographic inference

Table 5 summarizes posterior age estimates from BEAST analyses and biogeographic reconstructions for major lineages within *Crematogaster*. Divergence estimates are presented as median node ages and 95% credibility intervals for the three different schemes for calibration 3; node labels refer to Fig. 3 and 5. For a more extensive list of results see Supplementary Table 2 in the electronic material.

3.2.1. Impact of calibrations on divergence estimates

Comparative analyses of BEAST trace files (.log) from analyses with and without ('empty alignment') sequence data show that posterior distributions for calibrations 3 and 4 are distinct from the respective assigned prior distributions, indicating that they are indeed informed by the data (see Supplementary Fig. 1a and b). Applying the three different prior age distributions has a proportionally very small effect on the posterior age distribution of the calibrated node, with a shift of the applied prior median of 5 ma resulting in a shift of the median of the posterior age distribution of 2–2.5 ma or less. Comparing prior and posterior distributions for calibration 1 (Suppl. Fig. 1c) and 2 (Suppl. Fig. 1d) shows that here the prior is greatly influencing the posterior age estimations, basically more or less returning the input values. Calibration–exclusion analyses further suggest that calibrations 1 and 2 have only minor effects on posterior age estimations across the phylogeny (not shown). If calibration 4 is excluded, ages become unreasonably ancient (not shown), indicating that a calibration point close to the root node is vital for the analyses to return plausible estimates. Lastly, excluding calibration 3, the shallow calibration within *Crematogaster* itself, results in about 7–12 ma younger age estimations across the *Crematogaster* phylogeny. All in all, these results indicate a prominent role of the prior for calibration 3; the differences in results for median posterior ages between analyses under the three prior schemes, however, range only between 0.4 and 4.6 ma. Age estimates given in the following represent median ranges summarizing all three calibration schemes (Table 5 and Supplementary Table 2).

3.2.2. Age estimations and diversification within the genus *Crematogaster*

The *Orthocrema* clade and the Global and Australo-Asian *Crematogaster* clade share a most recent common ancestor (MRCA) between 40.5 and 44.9 ma, which suggests that crown group *Crematogaster* arose in this timeframe in the mid-Eocene (Fig. 3 and Table 5). The latest common ancestors of the Global and the Australo-Asian *Crematogaster* clades then diverged ca. 32.7–36.5 ma in the late Eocene. All three major phylogenetic lineages within the genus *Crematogaster* originated roughly at the same time, with crown group estimates for the *Orthocrema* clade ranging from 25.6 to 30.2 ma, for the Australo-Asian clade 25.8–28.9 ma,

Table 5
Divergence age estimates and ancestral range reconstructions. Divergence age estimates and ancestral range reconstructions for major clades. A: Palearctic, B: Afrotropical, C: Malagasy, D: South-East Asia, E: Australia and Papua New Guinea region; [|] represents the range inheritance scenario inferred by the DEC model for the two lineages descending from the respective node; PP = posterior probability; rP = relative probability. See Section 2.6 for details on models and methods, and Section 2.5 for details on calibrations for divergence dating.

			BEAST						LAGRANGE			
			Calibration 3A		Calibration 3B		Calibration 3C		DEC-M1		DEC-M2	
Clade	Node	PP	Median	95%	Median	95%	Median	95%	Range	rP	Range	rP
Genus *Crematogaster*	247	1.0	40.5	36.0,45.1	42.4	37.8,47.3	44.9	42.2,50.0	[D|D] [CD|D]	0.597 0.107	[D|D] [BD|D]	0.515 0.295
Orthocrema clade	69	1.0	25.6	23.0,28.6	27.6	24.8,30.7	30.2	27.2,33.4	[C|D] [B|D] [D|D] [CD|D]	0.223 0.201 0.127 0.119	[B|D] [B|BD]	0.908 0.025
Global + Australo-Asian *Crematogaster*	246	1.0	32.7	28.9,36.7	34.3	30.3,38.5	36.5	32.2,41.0	[D|D] [BD|D]	0.753 0.179	[D|D] [BD|D]	0.785 0.127
Global *Crematogaster*	212	1.0	23.8	20.9,26.9	25.0	21.9,28.5	26.9	23.2,30.4	[BD|B] [D|D] [D|BD]	0.493 0.162 0.123	[D|D] [BD|D] [AD|D]	0.416 0.200 0.145
Australo-Asian *Crematogaster*	245	1.0	25.8	22.5,29.5	27.2	23.5,30.9	28.9	25.1,33.0	[D|D]	0.911	[D|D]	0.909
						Global extinction rate			0.0055		0.0066	

and a few years younger for the Global *Crematogaster* clade with 23.8–26.9 ma.

Lineage-through time plots suggest a very low net lineage diversification rate for *Crematogaster* until ca. 25 ma (Fig. 4). After this time lineage diversity increases significantly, but roughly at a constant rate until reaching a plateau ca. 2–3 ma.

3.2.3. Dispersal history of the genus Crematogaster

The global extinction rates inferred by the DEC-models are low (M1: 0.0055; M2: 0.0066), suggesting that local extinction has not played a major role in the evolution of *Crematogaster* ants. Extinction rates, however, are known to be often underestimated by the DEC-model (Ree and Smith, 2008; Ronquist and Sanmartín, 2011), so these results should be viewed with caution.

The biogeographic history of the genus appears highly complex and shows evidence of numerous dispersal events between continents. Both DEC-models (M1 and M2) reconstruct South-East Asia as the most probable ancestral region for the genus *Crematogaster* (node 247, Fig. 3 and Table 5). The subsequent evolution and diversification of the genus into the three major lineages took place exclusively in S-E Asia and lasted for at least 15 ma. In the late Oligocene the three major lineages then embark on independent dispersal histories, commencing with the first dispersal of the *Orthocrema* clade out of S-E Asia. Descriptions of results in the following focus on the DEC-model M2 otherwise explicitly stated; for results of the DEC-M1 analysis refer to Supplementary Table 2.

3.2.3.1. Orthocrema clade. Overall biogeographic inference within the *Orthocrema* clade is less well supported than for the remainder of the phylogeny. Some relationships in this part of the tree were unstable between MrBayes (Fig. 2) and BEAST analyses (see Section 3.1.1) and biogeographic analyses may be compromised by this phylogenetic uncertainty.

A summary of results is depicted in Fig. 3a. Well supported is an initial geographic split in the history of the *Orthocrema* clade, with one lineage remaining in S-E Asia, while the other lineage disperses to the Afrotropical region sometime in the late Oligocene, between 22.3 and 30.2 ma (node 69 to 35). A subsequent dispersal event is inferred from Africa to the Neotropics ca. 19.5–25.9 ma (node 34 to 33), and also from Africa to Madagascar (node 14 to 13; 14.8–22.0 ma).

The other *Orthocrema* lineage remained in S-E Asia (node 68) until dispersal into the Neotropics (6.9–15.6 ma; node 48 to 46) and dispersal to the Australasian region (node 68 to 67). The latter event has good support, but the timeframe remains undefined (before 6.7 ma) given the long branch separating this primarily New Guinean lineage from the rest of S-E Asian lineage. A second independent dispersal of S-E Asian *Orthocrema* to Australasia occurred furthermore sometime after 7.9 ma (node 55). The 'S-E Asia to Neotropics' dispersal (node 48 to 46) receives low support (rP = 0.276), and almost equally supported is an alternative dispersal from S-E Asia to the Nearctic region (rP = 0.264; see Suppl. Table 2). The subsequent inferred move of *Orthocrema* from the Neotropics into the Nearctic remains also doubtful due to this circumstance (node 46).

3.2.3.2. The global Crematogaster clade. The evolutionary history of the Global *Crematogaster* clade is quite complicated, but major movements between geographical regions are sketched out in the following and in Fig. 3b. The MRCA of the Global clade (node 212) is inferred to have resided in S-E Asia and there diverged into two lineages, although this reconstruction has only a moderate relative probability (rP = 0.42, Table 5) and one of these lineages (node 211) has low phylogenetic support (see Fig. 2, and Suppl. Table 2). According to the reconstructed scenario (see Fig. 3b), the onset of dispersal of the Global clade out of S-E Asia is placed in the early Miocene. At that time, one major lineage of the Global clade spread first into the Afrotropical (15.5–21.4 ma; node 146 to 145), and then onwards into the Palearctic region (6.6–17.6 ma; node 145 to 144). Two more dispersal events to the Afrotropical region took place in the mid to late Miocene (9.9–13.9 ma, node 210 to 208 and node 198 to 190). Furthermore, three separate dispersals to the Australasian region from S-E Asia are supported, taking place sometime between 13.9 ma and the present (nodes 80 to 79, 210 to present, 197 to present). The Nearctic region was colonized by a single Palearctic ancestor fairly recently, 5.2–7.4 ma (node 144 to 140). Lastly, a recent dispersal from Africa back to S-E Asia sometime around or after 6.6 ma is inferred (node 206 to present).

3.2.3.3. Australo-Asian Crematogaster clade. In contrast, the biogeographic history of the Australo-Asian *Crematogaster* clade is simple. This lineage evolved entirely in S-E Asia until at least 20.5 ma, when a single colonization of the adjacent Australasian region is suggested (node 230 to 228; Fig. 3c) for the early to mid-Miocene (13.9–20.5 ma).

3.2.4. Colonization of Madagascar

Madagascar was colonized by acrobat ants through eight successive dispersal events (Fig. 5) by members of the *Orthocrema* and the *Global Crematogaster clade*. The dating analysis supports that an ancestral species within the *Orthocrema* clade was the first *Crematogaster* to arrive on the island. Biogeographic reconstructions suggests two independent dispersal events to Madagascar from Africa in the early to middle Miocene, one by an ancestor of *C. rasoherinae* (1; <26.8 ma) and one by an ancestor of the *C. volamena* and *C. madecassa*-groups (2; 14.8–22.0 ma) (Fig. 5a).

Further indicated is that Malagasy members of the *Global Crematogaster* clade have reached the island from continental Africa in the late Miocene and Pliocene (Fig. 5b and c). The enigmatic *C. ranavalonae*-group (3), former subgenus *Oxygyne* (see Blaimer, 2012a), is estimated to have arrived in Madagascar 5.6–9.5 ma. Other colonization events happened fairly rapidly within the same timeframe: The *C. degeeri-sewellii*-group (4), *C. hova*-group (6) and *C. kelleri*-group (7) are estimated to have reached the island around 5–6.0 ma, 5.5–8.8 ma and before 5.0 ma (but after 16.1 ma),

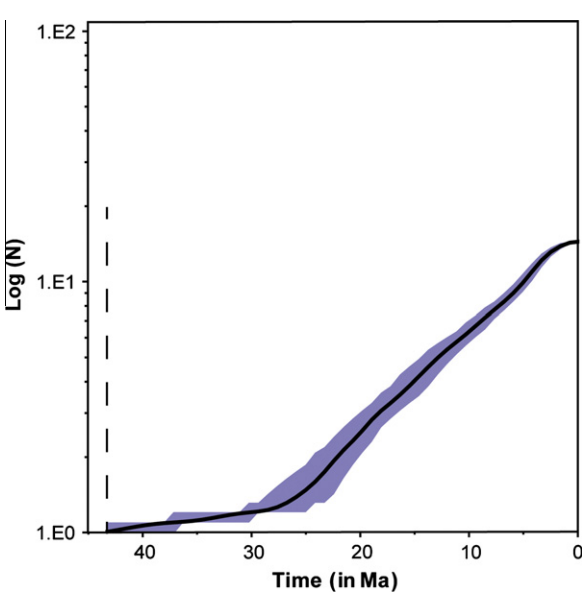

Fig. 4. Lineage diversification in *Crematogaster* through time. Lineage through time analysis was performed on results from BEAST analyses under calibration scheme 3B. The solid black line corresponds to the mean of the posterior probability density and the shaded area around it represents the 95% credible interval. The dashed vertical line marks the evolution of *Crematogaster*.

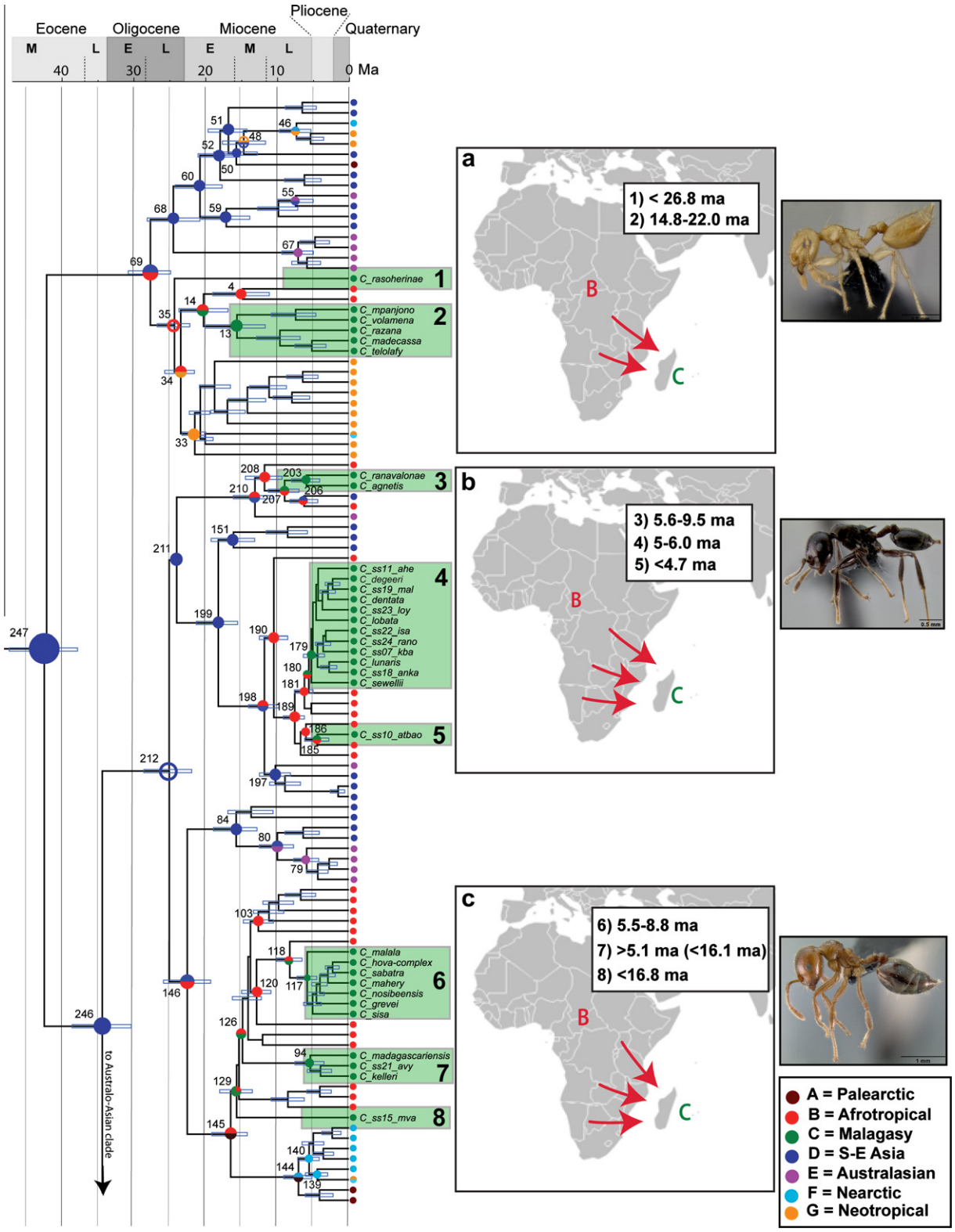

Fig. 5. Colonization of Madagascar by *Crematogaster*. Phylogeny and ancestral range inheritance scenarios on nodes are the same as in Fig. 3. Outgroups and the Australo-Asian *Crematogaster* clade have been pruned, and taxon labels for all non-Malagasy taxa have been deleted. Diagrams a, b and c summarize the dispersal history of *Crematogaster* to Madagascar as inferred by the DEC-M2 model. 1: *C. rasoherinae*, 2: *C. volamena*- and *C. madecassa*-groups, 3: *C. ranavalonae*-group, 4: *C. degeeri-sewellii*-group, 5: *C. ss10*, 6: *C. hova*-group, 7: *C. kelleri*-group, 8: *C. ss15*.

respectively. Two phylogenetically isolated and currently still undescribed Malagasy *Crematogaster* species have not further diversified since their arrival, indicating that they are recent faunal contributions. In one case (5, Fig. 5b) the arrival is suggested for after 4.7 ma, whereas in the other case (8, Fig. 5c) the timeframe remains vague (<16.8 ma).

3.2.5. Comparison of inferences of DEC-M1 and M2 model

For brevity the results estimated under the DEC-M1are not illustrated, but can be found in Supplementary Table 2. Overall both DEC-models agree well on range reconstructions, but often with varying relative probabilities. In some cases the M1 model considers the 'top scoring scenario' of the M2-model, but with a slightly lower relative probability (e.g. node 48 or 69, Suppl. Table 2). Major disagreements between the results of DEC-M1 and M2 are only seen at node 34, 35, 48, 69, 210, 211 and 212 (Suppl. Table 2); these seem to result from the varying assumptions about dispersal frequencies that constitute these models (see Section 2.5 and Table 4).

4. Discussion

4.1. The evolutionary history of Crematogaster – patterns and causes

Time-calibrated phylogenies have enlightened our knowledge of ant evolution tremendously in recent years, both on a family- and subfamily-wide scale (Brady et al., 2006; Moreau et al., 2006; Ward et al., 2010), and also increasingly at the level of genera (Jansen et al., 2010; Moreau, 2008; Schultz and Brady, 2008). However, countless more questions on the evolutionary history of ants remain unanswered. Here I have attempted to shed light on one of these riddles, the evolution of the dominant and diverse acrobat ants.

This study supports the origin of the genus *Crematogaster* somewhere in South-East Asia in the mid-Eocene. When analyzing geographic distribution patterns of ant genera across the Old World and New World tropics, Brown (1973) had hypothesized a "tropical Africa or southern Asia" origin for *Crematogaster* and other "world-dominating" genera such as *Pheidole*. He also was not far off in his suggestion for the timeframe of the spread of these dominant genera across the world, indicating they dispersed explosively across the world from the Miocene onwards (Brown, 1973). The present results support an increase in lineage diversity from ~25 ma (Fig. 4) in the late Oligocene onwards, after the three major *Crematogaster* lineages had evolved and the onset of dispersal out of S-E Asia began. The intriguing questions concerning the early evolution of *Crematogaster* now are (1) what factors drove the deep lineage diversification in S-E Asia? And then (2) what spurred or facilitated the subsequent onset of global spread from S-E Asia?

In the mid-Eocene, the composition of S-E Asian landmasses and islands was much more fragmented than in the present day (Hall, 2002). It is therefore possible that *Crematogaster* first evolved in a quite isolated part of this region. Dramatic geological changes occurred throughout the Cenozoic (<65 ma), as the Indian plate started to collide with the Eurasian plate in the north, while the Australian plate was moving northwards to collide with the latter in the south (Hall, 2002, 2009). The most significant tectonic rearrangements within S-E Asia are suggested for the late Oligocene to early Miocene period, between 20 and 30 ma (Hall, 1998), and thus interestingly fall within the same timeframe as the diversification of *Crematogaster* in S-E Asia (see Fig. 3). The geological changes increased topographical complexity of the region immensely; mountains began uplifting in Borneo only from the early Miocene on (Hall, 2009; Lohman et al., 2011). These events could have mediated vicariant speciation within *Crematogaster* through geographic isolation. Crame (2001) further links an overall pulse in species diversification in the tropics with a period of global warmth in the early Miocene (23–17 ma), following the cooler climates of the preceding Oligocene epoch. Acrobat ant diversification first of all may have also benefitted from these more favorable climatic conditions. Once the genus was reasonably diverse and widespread throughout S-E Asia, the probability of successful dispersal into other regions would have become elevated as well.

The first dispersal of *Crematogaster* from S-E Asia is here inferred to Africa during the time these paleogeologic and -climatic changes took place. A movement into Africa over land could have been facilitated first by the merging of India into Asia, and then further by Africa becoming adjacent to Eurasia in the early Miocene ~20 ma (Crame and Rosen, 2002). The possibility of transoceanic dispersal to Africa should not be discounted. The modern day equatorial system of ocean currents in the Indian Ocean only came into place since the drifting landmass of India crossed the equator northwards (Barron and Peterson, 1991), which until ca. 30–35 ma (Ali and Aitchison, 2008; Hall, 1998) deflected westwards flowing ocean currents southwards. With the subequatorial current established sometime after that, a first transoceanic dispersal event westwards to Africa would have become more probable. In any case, the onset of the 11 or 12 initial dispersal events out of South-East Asia in the early Miocene is both concurrent with the increasing connectivity of landmasses in the region and a more beneficial ocean current system able to support transoceanic dispersal. Considering the growing literature on transoceanic rafting events inferred for mammals and other vertebrates (e.g. Poux et al., 2005; Rocha et al., 2006; Townsend et al., 2011), dispersal through rafting by small insects such as arboreal twig-nesting ants seems quite plausible.

Particularly the biogeographic reconstructions within the *Orthocrema* clade have been compromised by topological uncertainty, with alternate topologies proposed by the different phylogenetic inference methods (see Section 3.1.1). Key taxa or lineages missing from the phylogeny could prevent correct biogeographic reconstructions and may cause inference of some curious long distance dispersal events, such as the transoceanic dispersal from S-E Asia to the Neotropics (Fig. 3a). An alternative scenario for this event would be a dispersal route northwards to the Palearctic and then across the Atlantic Ocean (or eastwards across the Bering Strait) into the Nearctic and Neotropics (as depicted by dashed arrows in Fig. 3a). *Crematogaster flavosensitiva* and *C. sumichrasti* have been somewhat arbitrarily coded as "Neotropical" but they are confined to Central America, with related taxa occurring in Mesoamerica and the southern Nearctic region. *Crematogaster sordidula* further is the only described Palearctic species within the *Orthocrema*, but *C. osakensis* has a northerly Asian distribution that could potentially extend somewhat into region A (see Fig. 1). Given these taxon distributions, a Palearctic–Nearctic–Neotropical route seems more plausible for this clade (node 50, Fig. 3).

The second dispersal of *Orthocrema* from the Afrotropical region into the Neotropics (Fig. 3a) in the early Miocene is well supported and can only be explained by transoceanic dispersal. A westwards transatlantic dispersal from Africa to the New World has also been suggested for plathyrrine monkeys (Houle, 1998; ~35 ma, Schrago and Russo, 2003), for scincid lizards (after 9 ma, Carranza and Arnold, 2003) and a diversity of plant families (Renner, 2004), presumably facilitated by the south-equatorial current (Renner, 2004).

Furthermore, the results suggest that there were only two colonizations of the Neotropics by *Orthocrema*, and most of the exceptional Neotropical *Crematogaster* diversity was generated by the latter dispersal event from the Afrotropics (see Fig. 3a). While there are some Neotropical species within the global *Crematogaster* clade, these are the small minority and evidently represent recent invasions from North America (see Fig. 3b). Also noteworthy is the single colonization of the Nearctic region within the Global clade by a fairly recent (5.2–7.4 ma) Palearctic ancestor. The Bering landbridge existed until just about this time (4.8–7.4 ma; Marincovich and Gladenkov, 1999), and this connection was recently used to explain the dispersal of lyceanid butterflies to the Nearctic region (Vila et al., 2011). This journey would have required a cold tolerance seen in only few extant species of *Crematogaster* (see Vila et al., 2011), but nonetheless this route could be equally probable

as yet another long-distance dispersal event across the Atlantic Ocean into the Nearctic region.

Three more dispersal events from S-E Asia to Africa are postulated for the Global clade, which may either have happened over water or by land. Most of the S-E Asian species placed in the Global *Crematogaster* clade in this study have either widespread or northwestern Asian distributions (i.e. India, Thailand), therefore an invasion of Africa via land seems most likely. Colonizations of the Australasian region by acrobat ants originated across all three major clades exclusively from S-E Asia (Fig. 3), but at least six times after 20.5 ma. These events were probably facilitated by the two regions becoming ever more connected (Hall, 2009).

Most of the here studied species of the Australo-Asian lineage are of southernmost Asian distribution. This lineage diversified greatly in Malaysia, New Guinea and Australia, but never took the leap into other biogeographic regions. This seems odd since the lineage is of similar age as the *Orthocrema* clade and the Global *Crematogaster* clade. Some of the members of the Australo-Asian clade are known to form associations with plants (e.g. Feldhaar et al., 2003; Quek et al., 2007), and maybe this more specialized life history prevented successful invasion of new habitats within this clade.

Despite this low frequency of dispersal within the Australo-Asian clade, the results overall suggests that most *Crematogaster* ants are extraordinary capable dispersers and colonizers, and one can only speculate about the characteristics that have facilitated its global spread. Their predominantly arboreal nesting habits for example could predispose them for successful transoceanic dispersal along with floating plant material more than ground-dwelling ants. Another advantage for successful dispersal and colonization of new regions could be the generally large size of *Crematogaster* colonies and the large body size of queens, which would elevate survival probabilities.

4.2. Colonization of Madagascar

A close-up examination of the colonization history of Madagascar by ants had previously been lacking, despite the recent proliferation of molecular studies on Malagasy taxa and their origins (e.g. Fuller et al., 2005; Poux et al., 2005, 2008; review by Yoder and Nowak, 2006). In comparison to the convoluted biogeographic history of the genus itself, the evolution of *Crematogaster* in the Malagasy region gives a much simpler picture (Fig. 5). Africa is the main source for acrobat ant species diversity in Madagascar. These results are unsurprising as African affinities have been found for other arthropods (e.g. Fuller et al., 2005; Kuntner and Agnarsson, 2011) and most vertebrates (e.g. Vences et al., 2003; Yoder et al., 2003). However, Madagascar also has distinct Asian faunal elements, recently reviewed by Warren et al. (2010), and in a few cases the Malagasy ant fauna also suggests these Asian affinities (Fisher, 2003). An alternative Asian range, instead of the weakly supported ancestral Afrotropical range, for the MRCA of *C. rasoherinae* and its sister clade (node 35; Fig. 3 and Suppl. Table 2) should therefore not be entirely discounted. This will, however, need to be investigated with increased taxon sampling, especially from the two regions in question.

The surprising aspect in Malagasy *Crematogaster* biogeography is hence not their origin, but the high frequency (eight times) of inferred dispersal events from Africa, which happened mostly within a relatively short time period in the late Miocene (Fig. 5). A recent taxonomic study focusing on Malagasy *Orthocrema* species moreover suggests that the *C. volamena* and *C. madecassa* species-groups are not sister groups and thus may have also reached Madagascar independently (Blaimer, 2012b). This dispersal frequency is unrivaled by any other published studies on Malagasy biogeography – therefore begging again the question what factors facilitated this mostly one-way biotic exchange? The late timeframe for most events can probably be correlated with a late establishment of the Global *Crematogaster* clade in Africa. Only after the genus was already quite abundant and diverse in Africa would dispersal to Madagascar have become more likely. Transoceanic rafting to Madagascar from Africa has been proposed even for lemurs (Kappeler, 2000). This is thought to have been assisted by a favorable system of oceanic currents in the Mozambique Channel operating before and probably throughout most of the early Miocene (Ali and Huber, 2010), flowing eastwards from Africa to Madagascar. When Madagascar on its northwards journey entered the tradewind zone, however, this pattern was reversed to the present day configuration, making oceanic dispersal from Africa to Madagascar much less likely from the mid Miocene onwards (Ali and Huber, 2010; Stankiewicz et al., 2006). Most colonization events of Madagascar by *Crematogaster* are estimated to have taken place in the late Miocene and could thus not have been facilitated by favorable ocean currents. Interestingly, the Comoros islands are currently estimated to have formed in the late Miocene (Rabinowitz and Woods, 2006) and thus could have provided a stepping stone land bridge for acrobat ant dispersal to Madagascar. This scenario appears quite plausible for the Malagasy taxa and species-groups that are presently shared with the Comoros islands, the *C. degeeri-sewellii*-group, *C. rasoherinae* and *C*_ss10 (Fig. 5; lineages 4, 1, 5 respectively), but in the case of the remaining taxa would need to assume extinction on the Comoros islands subsequent to the colonization of Madagascar.

Could the observed biogeographic patterns also have been created, at least in part, by a Malagasy source species pool dispersing multiple times to Africa instead of vice versa? This was for example shown to pertain for chameleons (Raxworthy et al., 2002). For *Crematogaster* this alternative is much less likely given the biogeographic history of the genus in other parts of the world, and its comparatively late arrival in Madagascar. The cohesive membership of most Malagasy species to distinct endemic clades, but which are scattered across most of the phylogeny, argues further for dispersal towards Madagascar and subsequent speciation. I realize, however, that these phylogenetic patterns could be altered by a more extensive taxon sampling in the Afrotropical region and then may need to be interpreted differently. 129 species of *Crematogaster* are currently described for the African continent (Bolton, 1995), of which only 24 were included in this study. The taxonomy of most African *Crematogaster* species is in need of revision, making it difficult to obtain samples, and current species numbers probably do not reflect the true species diversity. Nevertheless, the results presented here for the Malagasy *Crematogaster* underline again the exceptional role that transoceanic dispersal has played in the success of the genus on a global scale.

4.3. Phylogenetic structure and implications for subgeneric classification

The subgeneric classification of *Crematogaster* has long been considered insufficiently defined and was suspected to consist of artificial groupings (Longino, 2003; Brown, 1973). Changes have been overdue, but the necessary phylogenetic framework was lacking. Indeed, most of the previous15 subgenera have been shown to be not monophyletic in this study. Based upon this overview of the phylogenetic structure of the genus I have presented here, the current classification can be revised and the results provide a robust framework for future morphological and molecular studies of *Crematogaster* ants. Morphological results and the formal revision of the classification are, however, discussed elsewhere (Blaimer, in press), since they exceed the scope of this paper.

5. Conclusion

This time-calibrated molecular phylogenetic framework for *Crematogaster* has opened an exciting window into the evolution of one of the most species-rich groups of ants in the world. Most previous subgenera were found to be not monophyletic; instead three deeply divergent major clades were revealed that provide the basis for a revised internal classification reflecting the phylogenetic structure of the genus. Acrobat ants originated in the mid-Eocene in the S-E Asian region, where they diversified into the three lineages by the end of the Oligocene. This early evolutionary history is suggested to have been shaped extensively by tectonic and geological processes. The more recent evolution of the genus was marked by an onset of dispersal out of S-E Asia into other parts of the world in the early Miocene. These successful colonization events can be linked to both an increased connectivity of S-E Asia with other regions, as well as to an elevated probability of transoceanic dispersal along newly established ocean current systems. The frequency and distances of the inferred range movements beg the question of which characteristics predispose *Crematogaster* ants to being exceptionally good dispersers and colonizers. A comprehensive phylogenetic study for Madagascar has shown the *Crematogaster* species diversity on the island to consist of relatively recent neoendemic elements, mainly derived from the African mainland in the late Miocene or Pliocene. The evolutionary context now available for acrobat ants should encourage the further gathering of basic biological information for a broader range of *Crematogaster* species, and thus enable intriguing studies of trait evolution, such as nesting habits and the development of mutualistic associations with other organisms. Eventually these advances will bring us closer to understanding why this particular group of ants has been so successful on a global scale.

Acknowledgments

Specimen donations and loans by the following people formed the basis of this study and were greatly appreciated: B.L. Fisher, P.S. Ward, J.T. Longino, M.L. Borowiec, M. Janda, A. Lucky, E.M. Sarnat, S. van Noort, H. Feldhaar, H. Bharti, S. Hosoishi, M. Leponce, S.P. Yanoviak, E.P. Economo, R. Clouse, P.J. Gullan, M.G. Branstetter, F. Hita-Garcia, G. Fischer and S.P. Cover. Field work in Madagascar was made possible by the gracious help of Madagascar National Parks, B. Rajemison, T. Razafindrabe and M. Rajaonarivo. This paper was much improved by comments from P.S. Ward, P.J. Gullan, A. Lucky, B.L. Fisher and one anonymous reviewer. For providing access to museum collections for morphological work I thank B.L. Fisher, B. Merz, D. Burckhardt, J. Schuberth, F. Koch, P.S. Ward, S.P. Cover, G. Alpert and R. Poggi. Funding for this research was provided by the Entomology Department at UC Davis, the Jastro Shields Research Award, the Center for Population Biology at UC Davis, the Ernst Mayr travel award, and the National Science Foundation (DDIG-DEB-1107515 awarded to B.B. Blaimer and P.S. Ward; DEB-0842204 to P.S. Ward; DEB-0849982 to B.L. Fisher).

Appendix A. Supplementary material

Supplementary data associated with this article can be found, in the online version, at http://dx.doi.org/10.1016/j.ympev.2012.06.028.

References

Ali, J.R., Aitchison, J.C., 2008. Gondwana to Asia: plate tectonics, paleogeography and the biological connectivity of the Indian sub-continent from the middle Jurassic through latest Eocene (166–35 Ma). Earth-Sci. Rev. 88, 145–166.

Ali, J.R., Huber, M., 2010. Mammalian biodiversity on Madagascar controlled by ocean currents. Nature 463, 653–656.

Barron, E.J., Peterson, W.H., 1991. The Cenozoic ocean circulation based on ocean general circulation model results. Palaeogeogr. Palaeoclimatol. Palaeoecol. 83, 1–28.

Blaimer, B.B., 2010. Taxonomy and natural history of the *Crematogaster* (*Decacrema*) group in Madagascar. Zootaxa 2714, 1–39.

Blaimer, B.B., 2012a. Untangling complex morphological variation: taxonomic revision of the subgenus *Crematogaster* (*Oxygyne*) in Madagascar, with insight into the evolution and biogeography of this enigmatic ant clade (Hymenoptera: Formicidae). Syst. Entomol. 37, 240–260.

Blaimer, B.B., in press. A subgeneric revision of *Crematogaster* and discussion of regional species-groups (Hymenoptera: Formicidae). Zootaxa.

Blaimer, B.B, 2012b. Taxonomic revision and species-groups of the subgenus Crematogaster (Orthocrema) in the Malagasy region (Hymenoptera, Formicadae). Zookeys 199, 23–70.

Bolton, B., 1995. A taxonomic and zoogeographical census of the extant ant genera (Hymenoptera: Formicidae). J. Nat. Hist. 29, 1037–1056.

Bolton, B., 2003. Synopsis and classification of Formicidae. Mem. Am. Entomol. Inst. 71, 1–370.

Bolton, B., 2011. Bolton's Catalogue and Synopsis. <http://gap.entclub.org/> (accessed October 2011).

Brady, S.G., Schultz, T.R., Fisher, B.L., Ward, P.S., 2006. Evaluating alternative hypotheses for the early evolution and diversification of ants. Proc. Natl. Acad. Sci. USA 103, 18172–18177.

Brown, J.M., Lemmon, A.R., 2007. The importance of data partitioning and the utility of Bayes factors in Bayesian phylogenetics. Syst. Biol. 56, 643–655.

Brown, W.L., 1973. A comparison of the Hylean and Congo-West African rain forest ant faunas. In: Meggers, B.J., Ayensu, E.S., Duckworth, W.D. (Eds.), Tropical Forest Ecosystems in Africa and South America: A Comparative Review. Smithsonian Institution Press, Washington, DC, pp. 161–185.

Burnham, K.P., Anderson, D.R., 2002. Model selection and multimodel inference. a practical information theoretical approach. Springer, New York.

Carranza, S., Arnold, E.N., 2003. Investigating the origin of transoceanic distributions: mtdna shows *Mabuya* lizards (Reptilia, Scincidae) crossed the Atlantic twice. Syst. Biodivers. 1, 275–282.

Crame, J.A., 2001. Taxonomic diversity gradients through geological time. Divers. Distrib. 7, 175–189.

Crame, J.A., Rosen, B.R., 2002. Cenozoic palaeogeography and the rise of modern biodiversity patterns. Geological Society, London, Special Publications 194, 153–168.

Dejean, A., Fisher, B.L., Corbara, B., Rarevohitra, R., Randrianaivo, R., Rajemison, B., Leponce, M., 2010. Spatial distribution of dominant arboreal ants in a malagasy coastal rainforest: gaps and presence of an invasive species. PLoS One 5, e9319.

Dlussky, G.M., 1997. Genera of ants (Hymenoptera: Formicidae) from Baltic amber. J. Paleontol. 31, 616–627.

Drummond, A.J., Rambaut, A., 2007. BEAST: Bayesian evolutionary analysis by sampling trees. BMC Evol. Biol. 7, 214.

Edgar, R.C., 2004. MUSCLE: multiple sequence alignment with high accuracy and high throughput. Nucleic Acids Res. 32, 1792–1797.

Feldhaar, H., Fiala, B., Hashim, R., Maschwitz, U., 2003. Patterns of the *Crematogaster–Macaranga* association: the ant partner makes the difference. Insectes Soc. 50, 9–19.

Fisher, B.L., 2003. Formicidae, ants. In: Goodman, S.M., Benstead, J.P. (Eds.), The Natural History of Madagascar. The University of Chicago Press, Chicago, pp. 811–819.

Fuller, S., Schwarz, M., Tierney, S., 2005. Phylogenetics of the allodapine bee genus *Braunsapis*: historical biogeography and long-range dispersal over water. J. Biogeogr. 32, 2135–2144.

Guénard, B., Weiser, M.D., Dunn, R.R., 2010. Ant Genera of the World. <http://www.antmacroecology.org/ant_genera/index.html> (accessed November 2011).

Hall, R., 1998. The plate tectonics of Cenozoic SE Asia and the distribution of land and sea. In: Hall, R., Holloway, J.D. (Eds.), Biogeography and Geological Evolution of SE Asia. Backhuys Publishers, Leiden, pp. 99–124.

Hall, R., 2002. Cenozoic geological and plate tectonic evolution of SE Asia and the SW Pacific: computer-based reconstructions, model and animations. J. Asian Earth Sci. 20, 353–431.

Hall, R., 2009. Southeast Asia's changing palaeogeography. Blumea 54, 148–161.

Heled, J., Drummond, A.J., 2012. Calibrated tree priors for relaxed phylogenetics and divergence time estimation. Syst. Biol. 61, 138–149.

Ho, S.Y.W., Phillips, M.J., 2009. Accounting for calibration uncertainty in phylogenetic estimation of evolutionary divergence times. Syst. Biol. 58, 367–380.

Hosoishi, S., Ogata, K., 2009. A taxonomic revision of the Asian endemic subgenus *Physocrema* of the genus *Crematogaster* (Hymenoptera: Formicidae). Zootaxa 2062, 15–36.

Hosoishi, S., Yamane, S., Ogata, K., 2010. Subterranean species of the ant genus *Crematogaster* in Asia (Hymenoptera: Formicidae). Entomol. Sci. 13, 345–350.

Houle, A., 1998. Floating Islands: a mode of long-distance dispersal for small and medium-sized terrestrial vertebrates. Divers. Distrib. 4, 201–216.

Jansen, G., Savolainen, R., Vepsalainen, K., 2010. Phylogeny, divergence-time estimation, biogeography and social parasite-host relationships of the Holarctic ant genus *Myrmica* (Hymenoptera: Formicidae). Mol. Phylogenet. Evol. 56, 294–304.

Kappeler, P.M., 2000. Lemur origins: Rafting by groups of hibernators? Folia Primatol. (Basel) 71, 422–425.
Kass, R.E., Raftery, A.E., 1995. Bayes factors. J. Am. Stat. Assoc. 90, 773–795.
Kuntner, M., Agnarsson, I., 2011. Biogeography and diversification of hermit spiders on Indian Ocean islands (Nephilidae: Nephilengys). Mol. Phylogenet. Evol. 59, 477–488.
Li, C., Lu, G., Ortí, G., 2008. Optimal data partitioning and a test case for ray-finned fishes (Actinopterygii) based on ten nuclear loci. Syst. Biol. 57, 519–539.
Lohman, D.J., de Bruyn, M., Page, T., von Rintelen, K., Hall, R., Ng, P.K.L., Shih, H.-T., Carvalho, G.R., von Rintelen, T., 2011. Biogeography of the Indo-Australian archipelago. Annu. Rev. Ecol. Evol. Syst. 42, 205–226.
Lomolino, M.V., Riddle, B.R., Brown, J.H., 2005. Biogeography. Sinauer Associates, Inc., Sunderland, Massachusetts.
Longino, J.T., 2003. The *Crematogaster* (Hymenoptera, Formicidae, Myrmicinae) of Costa Rica. Zootaxa 151, 1–150.
Maddison, D.R., Maddison, W.P., 2000. MacClade 4. Analysis of Phylogeny and Character Evolution. Sinauer Associates, Sunderland, Massachusetts.
Marincovich, L., Gladenkov, A.Y., 1999. Evidence for an early opening of the Bering Strait. Nature 397, 149–151.
McGuire, J.A., Witt, C.C., Altshuler, D.L., Remsen, J.V., 2007. Phylogenetic systematics and biogeography of hummingbirds: Bayesian and maximum likelihood analyses of partitioned data and selection of an appropriate partitioning strategy. Syst. Biol. 56, 837–856.
Miller, M.A., Pfeiffer, W., Schwartz, T., 2010. Creating the CIPRES science gateway for inference of large phylogenetic trees. In: Proceedings of the Gateway Computing Environments Workshop (GCE) New Orleans, LA, pp. 1–8.
Moreau, C.S., 2008. Unraveling the evolutionary history of the hyperdiverse ant genus *Pheidole* (Hymenoptera: Formicidae). Mol. Phylogenet. Evol. 48, 224–239.
Moreau, C.S., Bell, C.D., Vila, R., Archibald, S.B., Pierce, N.E., 2006. Phylogeny of the ants: diversification in the age of angiosperms. Science 312, 101–104.
Nylander, J.A.A., 2004. MrModeltest v2. Evolutionary Biology Centre, Uppsala University.
Nylander, J.A.A., Ronquist, F., Huelsenbeck, J.P., Nieves-Aldrey, J., 2004. Bayesian phylogenetic analysis of combined data. Syst. Biol. 53, 47–67.
Posada, D., Crandall, K.A., 1998. MODELTEST: testing the model of DNA substitution. Bioinformatics 14, 817–818.
Poux, C., Madsen, O., Glos, J., de Jong, W.W., Vences, M., 2008. Molecular phylogeny and divergence times of Malagasy tenrecs: Influence of data partitioning and taxon sampling on dating analyses. BMC Evol. Biol. 8, Article No.: 102.
Poux, C., Madsen, O., Marquard, E., Vieites, D.R., de Jong, W.W., Vences, M., 2005. Asynchronous colonization of Madagascar by the four endemic clades of primates, tenrecs, carnivores, and rodents as inferred from nuclear genes. Syst. Biol. 54, 719–730.
Quek, S.-P., Davies, S.J., Ashton, P.S., Itino, T., Pierce, N.E., 2007. The geography of diversification in mutualistic ants: a gene's-eye view into the Neogene history of Sundaland rain forests. Mol. Ecol. 16, 2045–2062.
Rabinowitz, P.D., Woods, S., 2006. The Africa–Madagascar connection and mammalian migrations. J. Afr. Earth Sci. 44, 270–276.
Rambaut, A., Drummond, A.J., 2007. Tracer v1.4 [upated to v1.5]. available at http://beast.bio.ed.ac.uk/Tracer.
Raxworthy, C.J., Forstner, M.R.J., Nussbaum, R.A., 2002. Chameleon radiation by oceanic dispersal. Nature (London) 415, 784–786.
Ree, R.H., Moore, B.R., Webb, C.O., Donoghue, M.J., 2005. A likelihood framework for inferring the evolution of geographic range on phylogenetic trees. Evolution 59, 2299–2311.
Ree, R.H., Smith, S.A., 2008. Maximum likelihood inference of geographic range evolution by dispersal, local extinction, and cladogenesis. Syst. Biol. 57, 4–14.
Renner, S., 2004. Plant dispersal across the tropical Atlantic by wind and sea currents. Int. J. Plant Sci. 165 (4 Suppl.), S23–S33.
Rocha, S., Carretero, M.A., Vences, M., Glaw, F., James Harris, D., 2006. Deciphering patterns of transoceanic dispersal: the evolutionary origin and biogeography of coastal lizards (*Cryptoblepharus*) in the Western Indian Ocean region. J. Biogeogr. 33, 13–22.
Ronquist, F., 1997. Dispersal-vicariance analysis: a new approach to the quantification of historical biogeography. Syst. Biol. 46, 195–203.
Ronquist, F., Huelsenbeck, J.P., 2003. MRBAYES 3: Bayesian phylogenetic inference under mixed models. Bioinformatics 19, 1572–1574.
Ronquist, F., Sanmartín, I., 2011. Phylogenetic methods in biogeography. Annu. Rev. Ecol. Evol. Syst. 42, 441–464.
Schrago, C.G., Russo, C.A.M., 2003. Timing the origin of New World monkeys. Mol. Biol. Evol. 20, 1620–1625.
Schultz, T.R., Brady, S.G., 2008. Major evolutionary transitions in ant agriculture. Proc. Natl. Acad. Sci. USA 105, 5435–5440.
Stamatakis, A., 2006. RAxML-VI-HPC: maximum likelihood-based phylogenetic analyses with thousands of taxa and mixed models. Bioinformatics 22, 2688–2690.
Stankiewicz, J., Thiart, C., Masters, J.C., de Wit, M.J., 2006. Did lemurs have sweepstake tickets? An exploration of Simpson's model for the colonization of Madagascar by mammals. J. Biogeogr. 33, 221–235.
Storey, M., Mahoney, J.J., Saunders, D.A., Duncan, R.A., Kelley, S.P., 1995. Timing of the hot-spot related volcanism and the break-up of Madagascar and India. Science 267, 852–855.
Swofford, D.L., 2000. PAUP*. Phylogenetic Analysis Using Parsimony (*and other methods). Version 4. Sinauer Associates, Inc. Publishers, Sunderland, Massachussetts.
Townsend, T.M., Tolley, K.A., Glaw, F., Böhme, W., Vences, M., 2011. Eastward from Africa: palaeocurrent-mediated chameleon dispersal to the Seychelles islands. Biol. Lett. 7, 225–228.
Upchurch, P., 2008. Gondwanan break-up: legacies of a lost world? Trends Ecol. Evol. 23, 229–236.
Vences, M., Vieites, D.R., Glaw, F., Brinkmann, H., Kosuch, J., Veith, M., Meyer, A., 2003. Multiple overseas dispersal in amphibians. Proc. Roy. Soc. Lond. B Biol. Sci. 270, 2435–2442.
Vila, R., Bell, C.D., Macniven, R., Goldman-Huertas, B., Ree, R.H., Marshall, C.R., Bálint, Z., Johnson, K., Benyamini, D., Pierce, N.E., 2011. Phylogeny and palaeoecology of polyommatus blue butterflies show Beringia was a climate-regulated gateway to the New World. Proc. Roy. Soc. Lond. B Biol. Sci. 278, 2737–2744.
Ward, P.S., 2007. Phylogeny, classification, and species-level taxonomy of ants (Hymenoptera: Formicidae). Zootaxa 1668, 549–563.
Ward, P.S., Sumnicht, T.P., 2012. Molecular and morphological evidence for three sympatric species of *Leptanilla* (Hymenoptera: Formicidae) on the Greek island of Rhodes. Myrmecol. News 17, 5–11.
Ward, P.S., Brady, S.G., Fisher, B.L., Schultz, T.R., 2010. Phylogeny and biogeography of dolichoderine ants: effects of data partitioning and relict taxa on historical inference. Syst. Biol. 59, 342–362.
Ward, P.S., Downie, D.A., 2005. The ant subfamily Pseudomyrmecinae (Hymenoptera: Formicidae): phylogeny and evolution of big-eyed arboreal ants. Syst. Entomol. 30, 310–335.
Warnock, R.C.M., Yang, Z., Donoghue, P.C.J., 2011. Exploring uncertainty in the calibration of the molecular clock. Biol. Lett. http://dx.doi.org/10.1098/rsbl.2011.0710.
Warren, B.H., Strasberg, D., Bruggemann, J.H., Prys-Jones, R.P., Thébaud, C., 2010. Why does the biota of the Madagascar region have such a strong Asiatic flavour? Cladistics 26, 526–538.
Wilgenbusch, J.C., Warren, D.L., Swofford, D.L., 2004. AWTY: A system for graphical exploration of MCMC convergence in Bayesian phylogenetic inference. Available at http://ceb.csit.fsu.edu/awty.
Wilson, E.O., Hölldobler, B., 2005. The rise of the ants: a phylogenetic and ecological explanation. Proc. Natl. Acad. Sci. USA 102, 7411–7414.
Yang, Z., Rannala, B., 2006. Bayesian estimation of species divergence times under a molecular clock using multiple fossil calibrations with soft bounds. Mol. Biol. Evol. 23, 212–226.
Yoder, A.D., Burns, M.M., Zehr, S., Delefosse, T., Veron, G., Goodman, S.M., Flynn, J.J., 2003. Single origin of Malagasy carnivora from an African ancestor. Nature 421, 734–737.
Yoder, A.D., Nowak, M.D., 2006. Has vicariance or dispersal been the predominant biogeographic force in Madagascar? Only time will tell. Annu. Rev. Ecol. Evol. Syst. 37, 405–431.
Zwickl, D.J., 2006. Genetic Algorithm Approaches for the Phylogenetic Analysis of Large Biological Sequence Datasets under the Maximum Likelihood Criterion. Ph.D. thesis, The University of Texas at Austin.

Supplementary Table 1

Collection data of *Crematogaster* specimens included in the study including voucher number, collector, locality, GPS coordinates and the location of the voucher specimen.

Taxon	voucher specimen	collector	country	locality	LatDD	LongDD	Located
Crematogaster							
nosibeensis	CASENT0421564	Fisher,Griswold et al.	Madagascar	Antsiranana: Nosy Be, R.N.I. Lokobe, 6.3 km 112° ESE Hellville, 30m	-13.4193	48.3312	CASC
sisa	CASENT0127554	B.L.Fisher	Madagascar	Antsiranana: R.S. Manongarivo 17.3 km 218°SW Antanambao, 1580m	-14.0217	48.4183	CASC
sabatra	CASENT0193162	B.L.Fisher et al.	Madagascar	Fianarantsoa: P.N. Befotaka-Midongy, 28.5km S Midongy-Sud, 1250m	-23.8408	46.9575	CASC
mahery	CASENT0193469	B.B.Blaimer	Madagascar	Fianarantsoa: P.N. Andringitra; 15.7km Ambalamanenjana, 780m	-22.2235	47.0118	BBBC
malala	CASENT0421136	B.L.Fisher et al.	Madagascar	Fianarantsoa: P.C. Ankazomivady, 28,5 km SW Ambositra, 1780m	-20.7841	47.1670	CASC
grevei	CASENT0457634	Fisher,Griswold et al.	Madagascar	Toliara: R.S. Cap Sainte Marie, 14.9 km 261° W Marovato, 160m	-25.5944	45.1468	CASC
hova-complex	CASENT0058827	B.L.Fisher et al.	Madagascar	Toamasina: Forét Ambatovy, 14.3 km 57° Moramanga, 1075m	-18.8508	48.3200	CASC
liengmei	CASENT0193172	P.S.Ward	South Africa	Western Cape: Vrede, Anysberg Nature Reserve, 750m	-33.4667	20.5833	PSWC
lango	CASENT0090624	S.v.Noort	Central Afr. Rep.	Sangha-Mbaéré: P.N. Dzanga-Ndoki: Mabéa Bai, 21.4 km 53° NE Bayanga, 510m	3.0335	16.4095	CASC
borneensis	CASENT0193115	P.S.Cranston	Singapore	Central Catchment, Sime Road, (Site 53), 75m	1.3597	103.8100	BBBC
HFmsp10	CASENT0193611	H.Feldhaar	Malaysia	Sabah: Poring Hot Springs II, 500-800m	6.0500	116.7167	BBBC
decamera	CASENT0193613	D.Guicking	Malaysia	Sabah: Danum Valley, 180m	4.9648	117.8042	BBBC
ranavalonae	CASENT0193425	B.B.Blaimer	Madagascar	Toliara: P.N. Andohahela/parcel 1; 4.7km Tsimelahy, 470m	-24.9456	46.6805	BBBC
agnetis	CASENT0051228	B.L.Fisher	Madagascar	Toamasina: F Analamay, 1068m	-18.8062	48.3371	CASC
stadelmanni	CASENT0193573	S.v.Noort	Gabon	Ogoové-Maritime: Réserve des Monts Doudou, 24.3 km 307° NW Doussala, 350m	-2.2225	10.4058	CASC
santschii	CASENT0193640	S.v.Noort	South Africa	Kwazulu-Natal: Eastern shore of Lake Sibaya, 43m	-27.4124	32.7114	BBBC
meijerei	CASENT0193683	M.Janda	New Guinea	Sandaun: Ulai vill., 220m	-3.3845	141.5876	BBBC
aberrans	CASENT0193779	S.Hosoishi	India	Maharashtra: Sanjai Gandhi NP, 100-480m	19.2138	72.9199	BBBC
kelleri	CASENT0109989	B.L.Fisher et al.	Madagascar	Toamasina: Ile Sainte Marie, Forêt Kalalao, 9.9 km 34° Ambodifotatra, 100m	-16.9225	49.8873	CASC
ss21_avy	CASENT0058825	B.L.Fisher et al.	Madagascar	Toamasina: Forêt Ambatovy, 14.3 km 57° Moramanga, 1075m	-18.8508	48.3200	CASC
madagascariensis	CASENT0193580	B.L.Fisher et al.	Madagascar	Toliara: Forêt Ivohibe 55.6km N Tolagnaro, 650m	-24.5617	47.2002	CASC
ss10_atbao	CASENT0193221	B.B.Blaimer	Madagascar	Antsiranana: Antanambao; 23.9km N Ambanja, 55m	-13.8865	48.4979	BBBC
ss15_mva	CASENT0120279	B.L.Fisher et al.	Madagascar	Mahajanga: Maevatanana, 56m	-16.9482	46.8277	CASC
sewellii	CASENT0193579	B.L.Fisher et al.	Madagascar	Toamasina: Moramanga, 922m	-18.9442	48.2307	CASC
ss18_anka	CASENT0193039	B.B.Blaimer	Madagascar	RS Ankarana, 33km NW Ambilobe, 170m	-12.9171	49.1582	BBBC
lunaris	CASENT0110578	B.L.Fisher et al.	Madagascar	Antsiranana: Rés. Analamerana, 28.4 km 99° Anivorano-Nord	-12.7467	49.4948	CASC
ss07_kba	CASENT0148695	B.L.Fisher et al.	Madagascar	Toliara: R. S. Kalambatritra, Ampanihy, 1270m	-23.4635	46.4631	CASC
lobata	CASENT0193045	B.B.Blaimer	Madagascar	RS Ankarana, 33km NW Ambilobe, 170m	-12.9171	49.1582	BBBC
ss11_ahe	CASENT0193399	B.B.Blaimer	Madagascar	Toliara: PN Andohahela/parcel 3, Ankasofotsy, 4.5km Ranopiso, 160m	-25.0137	46.6465	BBBC
dentata	CASENT0193394	B.B.Blaimer	Madagascar	Toliara: P.N. Andohahela/parcel 3; Ankasofotsy; 3.9km Ranopiso, 170m	-25.0179	46.6518	BBBC
degeeri	CASENT0012764	B.L.Fisher et al.	Madagascar	Fianarantsoa: Ankazomivady, 28 km SSW Ambositra, 1670m	-20.7750	47.1683	CASC
ss19_mal	CASENT0021958	B.L.Fisher et al.	Madagascar	Toliara: Malaimbandy, 180m	-20.3432	45.5957	CASC
ss23_loy	CASENT0125705	B.L.Fisher et al.	Madagascar	Antananarivo: Kaloy, 1420m	-18.5900	47.6510	CASC
ss24_rano	CASENT0492850	B.L.Fisher et al.	Madagascar	Fianarantsoa: P.N. Ranomafana, 6.6 km 310° NW Ranomafana, 1150m	-21.2367	47.3967	CASC

ss22_isa	CASENT0491124	B.L.Fisher et al.	Madagascar	Fianarantsoa: P.N. Isalo, Ambovo Springs, 29.3 km 4° N Ranohira, 990m	-22.2983	45.3517	CASC
cf desperans	CASENT0193107	P.J.Gullan	South Africa	Eastern Cape: Orange Grove, East London, 120m	-33.0303	27.8443	BBBC
obnigra	CASENT0193112	E.M.Sarnat	Solomon Isl.	Guadalcanal Isl, Mt. Austen, 118m	-9.4556	159.9804	BBBC
fraxatrix	CASENT0193576	P.S.Ward	Malaysia	Sabah: Danum Valley, Nature Trail, 175m	4.9591	117.8018	BBBC
cf rogenhoferi	CASENT0193596	P.S.Ward	Malaysia	Sabah: Danum Valley Field Centre, 180m	4.9648	117.8042	BBBC
flava	CASENT0193691	H.Bharti	India	Himachal Pradesh: Paonta Sahib, 460m	30.5311	77.2967	BBBC
lineolata	CASENT0193619	P.S.Ward	Canada	Nova Scotia: Bedford, 10m	44.7170	-63.6758	BBBC
castanea	CASENT0193606	M.Leponce	Mozambique	Cabo Delgado: Atibo, 90m	-10.7068	40.2139	BBBC
cf ochracea	CASENT0193607	P.S.Ward	Malaysia	Sabah: Danum Valley Field Centre, 180m	4.9648	117.8042	BBBC
cf. laeviceps	CASENT0193616	P.S.Ward	Australia	QLD: 1km NW Cape Tribulation, 5m	-16.0667	145.4667	BBBC
ionia	CASENT0193617	L.Borowiec	Greece	Rhodes: road Kiotario-Asklipio, 300-500m Kiotari, 59m	36.0556	27.9472	BBBC
ss_AUS2	CASENT0193618	P. Gullan, Donaldson	Australia	ACT: Black Mountain, Canberra,	-35.2786	149.1004	BBBC
coarctata	CASENT0193116	B.B.Blaimer	U.S.A.	CA: Lake Co., McLaughlin Reserve, 650m	38.8500	-122.4167	BBBC
cf latuka	CASENT0193741	Robert O'Malley	Tanzania	Kigoma: Gombe NP, 790m	-4.7000	29.6167	BBBC
cf excisa	CASENT0193753	Georg Fischer	Kenya	Western Prov: Kakamenga NP, 1580m	0.3392	34.8617	BBBC
ss_TZ2	CASENT0193745	Robert O'Malley	Tanzania	Kigoma: Gombe NP, 790m	-4.7000	29.6167	BBBC
cf gerstaeckeri	CASENT0193739	Robert O'Malley	Tanzania	Kigoma: Gombe NP, 790m	-4.7000	29.6167	BBBC
subnuda	CASENT0193690	H.Bharti	India	Uttarakhand: Dehradun, 660m	30.3425	78.0607	BBBC
sagei	CASENT0193692	H.Bharti	India	Himachal Pradesh: Kotla, 500m	31.9190	75.9596	BBBC
flaviventris	CASENT0193696	J.Bezděk leg.	Yemen	Jabal Bura valley forest NP, Al Hudayah, 240-350m	15.8733	43.4100	BBBC
fruhstorferi	CASENT0193728	M.Janda	Indonesia	Kalimantan: Long Jelet, Kayan river, Malinau region, 410m	2.6875	115.8060	BBBC
pilosa	CASENT0193165	P.S.Ward	U.S.A.	FL: Escambia Co., 2km ESE Fort Pickens, 2m	30.3233	-87.2700	BBBC
isolata	CASENT0193229	P.S.Ward	U.S.A.	AZ: Cochise Co., Southwestern Research Station, 1650m	31.8833	-109.2133	BBBC
marioni	CASENT0193063	B.B.Blaimer	U.S.A.	CA: Contra Co., Knobcone Point, Mt. Diablo SP, 550m	37.8467	-121.9033	BBBC
cf rufigena	CASENT0193746	Robert O'Malley	Tanzania	Kigoma: Gombe NP, 790m	-4.7000	29.6167	BBBC
scutellaris	CASENT0193796	L.Borowiec	Spain	Baleares, Mallorca: Hotel Dolce Farniente et vic., Cala d'Or, 14m	39.3736	3.2203	BBBC
opaca	CASENT0193770	J.T.Longino	Honduras	Olancho: PN La Muralla, 1500m	15.0971	-86.7368	BBBC
abrupta	CASENT0219566	E.P.Economo	Solomon Isl.	San Cristobal Isl., Makira, 2.9km SE Kirakira, 97m	-10.4633	161.9600	EPEC
ss_AUS3	CASENT0193798	E.P.Economo	Australia	QLD: 9 km E Mareeba, 410m	-16.9895	145.5012	BBBC
mjobergi	CASENT0193799	E.P.Economo	Australia	QLD: 9 km E Mareeba, 410m	-16.9895	145.5012	BBBC
ss_AUS5	CASENT0193800	E.P.Economo	Australia	QLD: Musgrave Park, downtown Brisbane, 10m	-27.4790	153.0170	BBBC
rothneyi	CASENT0193801	S.Hosoishi	Cambodia	Kampong Thom Prov.	12.9062	105.2195	BBBC
subcircularis	CASENT0193915	S.Hosoishi	Malaysia	Selangor: Ulu Gombak, 330m	3.3000	101.7833	BBBC
cf ferrarii	CASENT0193918	P.S.Ward	China	HK: N.T., Kadoorie Institute Shek Kong Centre, 210m	22.4287	114.1141	BBBC
cf cylindriceps	CASENT0193916	S.Hosoishi	Cambodia	Kampong Thom Prov.	12.9062	105.2195	SHC
madecassa	CASENT0068164	B.L.Fisher et al.	Madagascar	Toamasina: Res. Ambodiriana, 4.8 km 306°Manompana, 125m	-16.6723	49.7012	CASC
mpanjono	CASENT0056947	D.Lees	Madagascar	Antsiranana: Nosy-Be: Antsirambazaha, Hell-Ville, 143m	-13.4135	48.3113	CASC
razana	CASENT0193589	B.L.Fisher et al.	Madagascar	Toliara: RS Kalambatritra, 1365m	-23.4185	46.4583	CASC
telolafy	CASENT0492527	B.L.Fisher et al.	Madagascar	Fianarantsoa: Parc National d'Isalo, 29.2 km 351° N Ranohira, 500m	-22.3133	45.2917	CASC
volamena	CASENT0162194	B.L.Fisher et al.	Madagascar	Toamasina: RS Ambatovaky, Sandrangato river, 400m	-16.8175	49.2925	CASC
rasoherinae	CASENT0070841	B.L.Fisher et al.	Madagascar	Fianarantsoa: R.F. Agnalazaha, Mahabo, 42.9 km 215° Farafangana, 20m	-23.1938	47.7230	CASC
cf gavapiga	CASENT0193609	P.S.Ward	Malaysia	Sabah: Danum Valley, Nature Trail, 175m	4.9591	117.8018	BBBC

torosa	CASENT0193195	M.G.Branstetter	Guatemala	Zacapa: 7.5km NE Teculután, 460m	15.0444	-89.6777	BBBC
irritabilis	CASENT0193598	A.Lucky	New Guinea	Western Prov.: Muller Range, 45km SW Kopiago, 495m	-5.7291	142.2633	BBBC
formosa	CASENT0193615	P.S.Ward	Guatemala	Sololá: 3km SSE San Andrés Semetabaj, 2040m	14.7167	-91.1167	BBBC
mesonotalis	CASENT0193622	P.S.Ward	Australia	QLD: Cape York Peninsula, 5km ENE Lockerbie, 70m	-10.7667	142.5000	BBBC
reticulata	CASENT0193610	P.S.Ward	Malaysia	Sabah: Danum Valley, Coupe 88, 300m	4.9696	117.8372	BBBC
smithi	CASENT0193697	S.P.Cover	U.S.A.	Apache Co.: 0.3 mi. N.Jct, Rt.60 on Co.Rd 3140, 2090m	34.2768	-109.6922	BBBC
binghamii	CASENT0193689	H.Bharti	India	Uttarakhand: Dehradun, 660m	30.3425	78.0607	BBBC
flavomicrops	CASENT0193764	J.T.Longino	Honduras	Gracias a Dios: Las Marias, 370m	15.7184	-84.8781	BBBC
baduvi	CASENT0193723	M.Janda	Indonesia	East Kalimantan: Long Jelet, Kayan river, Malinau region, 410m	2.6875	115.8060	BBBC
longipilosa	CASENT0193780	S.Hosoishi	Malaysia	Selangor: Ulu Gombak, 330m	3.3000	101.7833	BBBC
ortho_CAR1	CASENT0414275	B.L.Fisher	Central Afr. Rep.	Sangha-Mbaéré: P.N. Dzanga-Ndoki, 39.6km 174ºS Lidjombo, 340m	2.3500	16.1500	CASC
sordidula	CASENT0193797	Borowiec,Poprawska	Croatia	N Dalmatia: Pakoštane, 40m	43.9167	15.5000	BBBC
nigropilosa	CASENT0193769	J.T.Longino	Honduras	Olancho: 14km WSW Catacamas, 600m	14.7997	-86.0142	BBBC
longispina	CASENT0193767	J.T.Longino	Costa Rica	Alajuela: Poco Sol, 800m	10.3456	-84.6744	BBBC
tenuicula	CASENT0193774	J.T.Longino	Costa Rica	Puntarenas: 15km SSW Pto. Jimenez, 170m	8.4080	-83.3276	BBBC
sumichrasti	CASENT0193773	J.T.Longino	Guatemala	Suchitepéquez: 5km S Vol. Atitlán, 1170m	14.5338	-91.1995	BBBC
osakensis	CASENT0193877	B.L.Fisher	China	Yunnan: Xishuangbanna Pref., Mengla County, Manzhuang village, 890m	21.4232	101.6890	CASC
fritzi	CASENT0193803	Clouse&Sharma	Micronesia	Pohnpei, Kepirohi Falls, FSM, 46m	6.8455	158.2992	BBBC
emeryi	CASENT0193805	M.Janda et al.	New Guinea	Madang, Baitabag vill., 75m	-5.1398	145.7751	BBBC
victima	CASENT0193878	A.V.Suarez	Argentina	Herradura, Formosa, 60m	-26.4976	-58.2897	BBBC
cf dolens	CASENT0193756	Joachim Schumann	Kenya	Western: Arabuko Sokoke Forest, 10m	-3.3247	39.9475	BBBC
ortho_TH1	CASENT0130762	Areeluck	Thailand	Chiang Mai: Doi Inthanon NP, Vachiratharn falls, 650m	18.5260	98.6008	CASC
quadriformis	CASENT0193881	A.V.Suarez	Argentina	Santa Fe: ~10km east of Villa Ocampo, 40m	-28.4980	-59.2651	BBBC
treubi	CASENT0193783	S.Hosoishi	Cambodia	Kampong Thom Prov.	12.7000	104.8833	BBBC
ss_TH1	CASENT0119409	Khampol, Jaidee	Thailand	Khonkaen: Nam Pong NP, 300m	16.6200	102.5747	CASC
paradoxa	CASENT0193114	E.M.Sarnat	New Guinea	Gulf Prov.: 11km SSE Haia airstrip, 800m	-6.8000	145.0167	BBBC
rhachio_PNG2	CASENT0193603	A.Lucky	New Guinea	Western Prov.: Muller Range, 36km SW Kopiago, 1310m	-5.6621	142.2966	BBBC
aculeata	CASENT0193600	K.Sagata	New Guinea	New Britain: Vouvou, 20km N Palmalmal II, 880m	-5.4431	151.4040	BBBC
arcuata	CASENT0193084	B.B.Blaimer	Venezuela	Aragua: Estacion Rancho-Grande, PN Henri Pittier, 1100m	10.5824	-68.4735	BBBC
corvina	CASENT0193759	B.E.Boudinot	Honduras	Francisco Morazán: E.A.P. Zamorano, 800m	14.0130	-87.0080	BBBC
acuta	CASENT0193650	P.S.Ward	Honduras	Atlántida: 9km S Yaruca, 950m	15.5831	-86.7267	BBBC
cf_wasmanni	CASENT0081166	B.L.Fisher	Central Afr. Rep.	Sangha-Mbaéré: P.N. Dzanga-Ndoki, 38.6 km 173° S Lidjombo, 350m	2.3600	16.1440	CASC
cf depressa	CASENT0087590	S.v.Noort	Central Afr.Rep.	Sangha-Mbaéré: P.N. Dzanga-Ndoki, 38.6 km 173° S Lidjombo, 350m	2.3600	16.1440	CASC
cf buchneri	CASENT0193750	G.Fischer	Kenya	Western Prov: Kakamenga NP, 1580m	0.3392	34.8617	BBBC
cf gabonensis	CASENT0193595	S.P.Yanoviak	Gabon	Ogooué-Maritime: Gamba, 50m	-2.7000	10.0000	BBBC
wellmani	CASENT0193751	G.Fischer	Kenya	Western Prov: Kakamenga NP, 1580m	0.3392	34.8617	BBBC
cf chlorotica	CASENT0415414	B.L.Fisher	Central Afr.Rep.	Sangha-Mbaéré: P.N. Dzanga-Ndoki, Mabéa Bai, 21.4 km 53° NE Bayanga, 510m	3.0333	16.4100	CASC
cf bequaerti	CASENT0193744	Robert O'Malley	Tanzania	Kigoma: Gombe NP, 790m	-4.7000	29.6167	BBBC
cf concava	CASENT0193755	G.Fischer	Kenya	Western Prov: Kakamenga NP, 1580m	0.3392	34.8617	BBBC
cf luctans	CASENT0193747	Robert O'Malley	Tanzania	Kigoma: Gombe NP, 790m	-4.7000	29.6167	BBBC
tetracantha	CASENT0193113	E.M.Sarnat	New Guinea	Gulf Prov.: 13km S Haia airstrip, 700m	-6.8167	145.0000	BBBC
dahlii	CASENT0193602	K.Sagata	New Guinea	New Britain: Vouvou, 20km N Palmalmal IV, 920m	-5.4400	151.4594	BBBC

weberi	CASENT0193599	K.Sagata	New Guinea	New Britain: Vouvou, 20km N Palmalmal II, 880m	-5.4431	151.4040	BBBC
modigliani	CASENT0193575	P.S.Ward	Malaysia	Sabah: Danum Valley, Orchid Trail, 180m	4.9636	117.8040	BBBC
coriaria	CASENT0193778	S.Hosoishi	Malaysia	Selangor: Ulu Gombak, 330m	3.3000	101.7833	BBBC
ampullaris	CASENT0193577	P.S.Ward	Malaysia	Sabah: Danum Valley, West Trail, 220m	4.9656	117.7994	BBBC
inflata	CASENT0193621	P.S.Ward	Malaysia	Sabah: Danum Valley, Nature Trail, 175m	4.9591	117.8018	BBBC
onusta	CASENT0193714	M.Janda	Indonesia	East Kalimantan: 30km N Balikpapan, Sungai Wain NP, Jamaludin camp, 100m	-1.0970	112.8228	BBBC

Supplementary Table 2

Results of divergence age estimates and ancestral range reconstructions. A: Palearctic region; B: Afrotropical region; C: Malagasy region; D: South-East Asia; E: Australia & Papua New Guinea region; F: Nearctic region; G: Neotropical region; [|] represents the range inheritance scenario inferred by the DEC model for the two lineages descending from the respective node; only scenarios with rel. prob. > 0.1 are shown. PP = posterior probability; rP = relative probability. See section 2.6 for details on models and methods, and section 2.5 for details on calibrations for divergence dating.

		BEAST						LAGRANGE			
		Calibration 3A		Calibration 3B		Calibration 3C		DEC-M1		DEC-M2	
node	**PP**	**median**	**95%**	**median**	**95%**	**median**	**95%**	**range**	**rP**	**range**	**rP**
4	1.0	13.9	10.3,17.67	14.8	11.06,18.94	15.9	11.79,20.59	[B|B]	0.875	[B|B]	0.953
13	0.98	14.8	11.2,19.26	15.6	11.64,20.0	16.6	12.36,21.2	[C|C]	0.942	[C|C]	0.897
14	0.78	18.7	15.57,21.78	20.2	16.81,23.65	22.0	17.96,25.88	[B|C]	0.713	[B|C]	0.744
								[C|C]	0.101	[B|B]	0.145
33	1.0	19.5	20.42,24.46	21.4	19.91,23.22	24.0	22.23,25.92	[G|G]	0.382	[G|G]	0.617
								[G|BG]	0.287	[G|BG]	0.326
								[G|DG]	0.192		
34	0.81	21.4	19.71,23.36	23.4	21.48,25.64	25.9	23.75,28.15	[BC|B]	0.343	[B|G]	0.511
								[C|D]	0.244	[BC|B]	0.285
								[B|G]	0.215	[B|B]	0.147
35	1.0	22.3	20.4,24.5	24.3	22.2,26.7	26.8	24.6,29.3	[C|CD]	0.256	[B|B]	0.362
								[C|BC]	0.194	[C|BC]	0.281
								[C|C]	0.148	[B|BG]	0.169
										[C|B]	0.130
46	1.0	6.9	4.96,8.99	7.3	5.28,9.66	7.8	5.51,10.27	[F|G]	0.665	[F|G]	0.827
								[D|G]	0.172		
48	0.80	13.8	11.03,16.7	14.6	11.6,17.61	15.6	12.27,19.1	[D|D]	0.362	[G|D]	0.276
								[F|D]	0.285	[F|D]	0.264
								[G|D]	0.275	[D|D]	0.179
										[A|D]	0.138
50	0.77	14.8	12.08,17.68	15.7	12.76,18.8	16.8	13.29,20.23	[D|D]	0.625	[D|D]	0.532
								[D|A]	0.222	[AD|A]	0.144
										[D|A]	0.141
51	0.55	15.8	13.31,18.67	16.8	14.19,19.6	17.9	14.82,20.98	[D|D]	0.918	[D|D]	0.860
52	0.96	16.9	14.23,19.77	17.9	15.17,20.99	19.2	15.00,22.54	[D|D]	0.969	[D|D]	0.947
55	0.99	7.0	4.77,9.59	7.4	4.96,10.0	7.9	5.26,10.8	[E|D]	0.780	[E|D]	0.750
								[D|D]	0.150	[D|D]	0.171
								[E|DE]	0.034	[E|DE]	0.040
59	0.91	16.2	13.07,19.61	17.1	13.79,20.54	18.2	14.62,21.93	[D|D]	0.811	[D|D]	0.881
								[DE|D]	0.179	[DE|D]	0.107
60	1.0	19.6	16.6,23.0	20.7	17.6,24.2	22.1	18.7,25.8	[D|D]	0.823	[D|D]	0.894
								[D|DE]	0.163		

67	1.0	6.7	4.83,9.07	7.1	4.95,9.32	7.4	5.13,9.94	[E|E]	0.937	[E|E]	0.933
68	0.92	22.8	19.57,26.21	24.4	20.73,28.06	26.3	22.3,30.33	[D|D]	0.399	[D|D]	0.543
								[D|E]	0.329	[D|E]	0.310
								[DE|E]	0.134		
69	1.0	25.6	23.0,28.6	27.6	24.8,30.7	30.2	27.2,33.4	[C|D]	0.223	[B|D]	0.908
								[B|D]	0.201	[B|BD]	0.025
								[D|D]	0.127		
								[CD|D]	0.119		
79	0.99	5.6	4.03,7.38	5.9	4.18,7.67	6.3	4.49,8.22	[E|E]	0.966	[E|E]	0.965
80	1.0	9.5	7.31,11.85	10.0	7.71,12.46	10.6	8.11,13.25	[D|E]	0.880	[D|E]	0.869
84	1.0	15.0	12.2,17.8	15.7	12.8,18.8	16.8	13.5,20.1	[D|D]	0.800	[D|D]	0.807
								[DE|D]	0.177	[DE|D]	0.167
94	1.0	5.1	3.25,7.16	5.4	3.46,7.49	5.8	3.72,8.1	[C|C]	0.967	[C|C]	0.943
103	1.0	11.9	9.94,13.08	12.6	10.5,14.68	14.9	12.66,17.11	[B|B]	0.999	[B|B]	0.999
117	1.0	5.5	4.19,6.85	5.8	4.47,7.21	6.2	4.81,7.78	[C|C]	0.978	[C|C]	0.974
118	1.0	7.7	6.07,9.51	8.2	6.52,10.06	8.8	6.97,10.79	[B|C]	0.907	[B|C]	0.888
120	0.77	12.1	10.1,14.17	12.8	10.84,14.92	13.6	11.44,15.9	[B|B]	0.782	[B|B]	0.855
								[BC|B]	0.212	[BC|B]	0.139
126	0.68	13.8	n/a	14.8	n/a	16.1		[C|B]	0.641	[C|B]	0.602
								[C|BC]	0.193	[B|B]	0.232
								[B|B]	0.122	[C|BC]	0.120
129	0.76	14.8	12.74,17.19	15.6	13.43,17.99	16.8	14.29,19.37	[BC|C]	0.772	[BC|C]	0.684
								[B|B]	0.129	[B|B]	0.251
139	1.0	4.2	2.78,5.66	4.4	2.94,6.04	4.7	3.09,6.43	[F|F]	0.944	[F|F]	0.946
140	0.95	5.2	3.9,6.71	5.5	4.12,7.12	5.8	4.31,7.54	[F|F]	0.978	[F|F]	0.982
144	1.0	6.6	4.92,8.57	7.0	5.14,9.06	7.4	5.35,9.58	[F|A]	0.882	[F|A]	0.946
145	1.0	15.5	13.4,18.1	16.4	14.1,19.0	17.6	14.9,20.4	[B|A]	0.359	[B|A]	0.815
								[B|F]	0.355		
146	1.0	21.4	18.3,24.4	22.5	19.2,25.8	24.1	20.6,27.6	[D|B]	0.645	[D|B]	0.520
								[D|D]	0.108	[D|A]	0.306
151	1.0	15.3	12.33,18.24	16.1	13.1,19.18	17.2	13.82,20.51	[D|D]	0.996	[D|D]	0.995
179	0.81	5.0	3.97,6.1	5.2	4.22,6.32	5.6	4.48,6.82	[C|C]	0.983	[C|C]	0.981
180	0.39	5.3	n/a	5.6	n/a	6.0	n/a	[B|C]	0.949	[B|C]	0.939
181	0.66	6.3	5.09,7.6	6.2	4.98,7.58	6.7	5.3,8.18	[B|B]	0.660	[B|B]	0.658
								[B|BC]	0.339	[B|BC]	0.339
185	1.0	4.2	2.61,5.81	4.4	2.78,6.15	4.7	2.91,6.53	[C|B]	0.811	[C|B]	0.787
								[B|B]	0.148	[B|B]	0.166
186	0.31	n/a		6.0	n/a	n/a		[B|B]	0.915	[B|B]	0.916
189	1.0	7.2	5.91,8.64	7.5	6.18,9.12	8.1	6.52,9.68	[B|B]	0.892	[B|B]	0.890
190	0.73	9.9	8.13,11.81	10.4	8.49,12.46	11.1	9.04,13.33	[B|B]	0.970	[B|B]	0.956
197	0.99	9.7	7.74,11.72	10.2	8.13,12.44	10.9	8.61,13.31	[D|D]	0.464	[D|D]	0.524
								[D|E]	0.412	[D|E]	0.427
198	1.0	11.1	9.2,13.2	11.8	9.7,14.0	12.5	10.3,15.0	[B|D]	0.867	[B|D]	0.937
199	1.0	17.3	14.6,20.2	18.2	15.5,21.2	19.4	16.3,22.6	[D|BD]	0.766	[D|D]	0.682
								[D|D]	0.196	[D|BD]	0.291
203	1.0	5.6	3.86,7.52	5.9	4.05,7.96	6.3	4.23,8.41	[C|C]	0.891	[C|C]	0.813
206	1.0	5.9	4.1,7.82	6.2	4.32,8.2	6.6	4.56,8.72	[D|B]	0.756	[D|B]	0.768

								[B|B]	0.151	[B|B]	0.156
207	1.0	8.5	6.61,10.55	8.9	6.93,11.21	9.5	7.3,11.76	[C|B]	0.721	[C|B]	0.635
								[B|B]	0.079	[B|BD]	0.218
208	0.99	11.1	8.94,13.65	11.7	9.3,14.4	12.5	9.98,15.24	[B|B]	0.771	[B|B]	0.665
										[B|BD]	0.204
210	1.0	12.4	10.0,15.0	13.1	10.6,16.1	13.9	11.1,17.0	[B|E]	0.607	[B|D]	0.528
								[B|B]	0.143	[D|E]	0.165
										[B|E]	0.118
211	0.45	22.8	n/a	24.0	n/a	25.7	n/a	[B|B]	0.496	[D|D]	0.738
								[BD|B]	0.258	[B|B]	0.124
								[D|D]	0.153		
212	1.0	23.8	20.9,26.9	25.0	21.9,28.5	26.9	23.2,30.4	[BD|B]	0.493	[D|D]	0.416
								[D|D]	0.162	[BD|D]	0.200
								[D|BD]	0.123	[AD|D]	0.145
228	1.0	13.9	11.47,16.7	14.7	12.04,17.51	15.5	12.65,18.55	[E|E]	0.889	[E|E]	0.891
230	0.93	18.3	15.4,21.47	19.4	16.22,22.75	20.5	17.03,24.07	[E|D]	0.704	[E|D]	0.671
								[D|D]	0.169	[D|D]	0.173
										[E|DE]	0.105
231	1.0	20.4	17.31,23.78	21.5	18.13,25.13	22.8	19.28,26.62	[D|D]	0.672	[D|D]	0.662
								[D|DE]	0.314	[D|DE]	0.309
244	0.99	22.8	19.34,26.55	23.9	20.29,27.94	25.5	21.59,29.83	[D|D]	0.996	[D|D]	0.991
245	1.0	25.8	22.5,29.5	27.2	23.5,30.9	28.9	25.1,33.0	[D|D]	0.911	[D|D]	0.909
246	1.0	32.7	28.9,36.7	34.3	30.3,38.5	36.5	32.2,41.0	[D|D]	0.753	[D|D]	0.785
								[BD|D]	0.179	[BD|D]	0.127
247	1.0	40.5	36.0,45.1	42.4	37.8,47.3	44.9	42.2,50.0	[D|D]	0.597	[D|D]	0.515
								[CD|D]	0.107	[BD|D]	0.295
							global extinction rate	**0.0055**		**0.0066**	

Supplementary data 2

Derivation of fossil calibrations

1) *Stenamma berendti* Mayr, a Baltic amber fossil, ca. 42 ma (Dlussky, 1997). This is a stem calibration placed on the node subtending *Stenamma dyscheres* and *Aphaenogaster occidentalis*. A lognormal prior distribution has been assigned with values of 42, 49.4 and 58.8, representing a hard lower bound, median and 95% soft upper bound respectively (input values: *zero offset*: *42, mean: 2.0* and *SD: 0.5*). This prior incorporates the notion that the most recent common ancestor (MRCA) of these two genera must have originated a considerable amount of time before the appearance of *Stenamma* in the Baltic amber fossil record.

2) *Temnothorax* spp. in Baltic amber (Dlussky, 1997), a stem calibration prior density placed on the MRCA of *Temnothorax rugatulus* and *Leptothorax muscorum*. Following the same reasoning as above a lognormal prior distribution was assigned to this node with values of 42, 49.4 and 58.8 (*42, 2.0, and 0.5*).

3) *Crematogaster crinosa*-group sp. in Dominican amber, ca. 17–20 ma. This is a fossil of a *Crematogaster* species that can be assigned based upon distinct morphological characters to the *C. crinosa* species-group (pers. observ.), as defined in Longino (2003). In this dataset, the *C. crinosa*-group is represented by *C. torosa*, and the fossil is assigned therefore as a stem calibration at the node subtending *C. torosa* and *C. longispina*, a species outside of the *C. crinosa*-group. Species within the *C. crinosa*-group are among the most common *Crematogaster* in the Neotropics (Longino, 2003) and may be fairly frequent in Dominican amber, but the ancestor of this group presumably originated some time before its appearance in the fossil record. *C. longispina* is morphologically quite different from the *C. crinosa*-group. One would therefore not expect the MRCA of *C. torosa* and *C. longispina* to be morphologically close to the *crinosa*-group, leading me to assume an age distribution for node 3 that somewhat predates the age of the amber fossil. I therefore assigned three different lognormal prior distribution to this node that together explore the biologically plausible age range for the MRCA of a stem *C. crinosa*-group: A) 17, 20.3 and 25.2 (input values: *zero offset*: *17, mean: 1.2* and *SD: 0.55*), B) 17, 25.2 and 30.4 (*17, 2.1* and *0.3*) and C) 17, 30.5 and 35.7 (*17, 2.6* and *0.2*).

4) Myrmicinae subclade containing *Crematogaster* and all outgroups except *Stenamma* and *Aphaenogaster*. A secondary calibration representing the crown-group age range for this clade as estimated in Brady et al. (2006) (S. Brady, pers. comm.; age for this node not published). I here assigned a normal distribution with lower bound = 56.6 ma and upper bound = 68.3 ma (input values: *mean: 62.45* and *SD: 3.45*) reflecting the range of estimates obtained in the previous study (S.Brady, pers. comm.).